cells. In contrast, at a high HA concentration (33 μg/mL, similar to Stab2$^{-/-}$ serum levels), tethering was significantly reduced (Fig. 5 *G* and *H* and Movies S1 and S2). These results indicate that a high level of HA in the circulation prevents the attachment of melanoma cells to the lung.

## Discussion

In this study, using Stab2 KO mice and an anti-Stab2 mAb, we provide several lines of evidence indicating that Stab2 is the major clearance receptor for circulating HA. This finding is consistent with the results of a previous in vitro study showing that Stab2, not its homolog Stab1, is the major clearance receptor for HA (5), as well as a recent study using Stab1 and Stab2 KO mice (2). In addition, KO mice deficient in either Lyve1 or Stab1 showed no change in serum HA levels (2, 29), further supporting this idea. Although Stab2 is known to bind other molecules, such as ac-LDL and heparin, serum levels of ac-LDL and heparin were not increased in the Stab2 KO mice, and the internalization of ac-LDL into Stab2-deficient HSECs was normal, indicating that those molecules are cleared by other scavenger receptors, such as Stab1. Therefore, we conclude that Stab2 is the bona fide clearance receptor for circulating HA in vivo.

An unexpected finding—and perhaps the most important result of this study—is the markedly reduced metastasis of melanoma cells in the Stab2 KO mice. Furthermore, i.p. administration of the blocking mAb for Stab2 also increased the serum concentration of HA and inhibited tumor metastasis in the Stab2$^{+/+}$ mice at levels comparable to those in Stab2 KO mice (Fig. 3). The KO mice were fertile, developed normally, and exhibited no hematological or histological changes except for the increased serum HA level (Fig. S1 and Table S1). Although Stab2 has multiple ligands, only HA levels were altered in the Stab2 KO mice, and the anti-Stab2 mAb caused phenotypes similar to those in the Stab2 KO mice. Thus, we focused on HA to investigate the mechanism preventing metastasis, and carried out various experiments in vitro and in vivo. Our in vitro experiments indicated that HA did not affect the proliferation, migration, and invasion of B16F10 cells (Fig. S3 *A–E*). Moreover, the weights of tumors formed by s.c. transplanted melanoma cells, as well as the cell cycle status of i.v. injected melanoma cells, were not changed in the Stab2 KO mice, indicating that the lack of Stab2 does not affect tumor proliferation in vivo (Fig. 2*C* and Fig. S3*B*). Likewise, mammary tumor cells formed primary tumors in abdominal fat pads, but tumor formation in the lymph nodes or lung was severely suppressed by anti-Stab2 mAb (Fig. 4). These results strongly suggest that tumor metastasis is prevented by a mechanism other than proliferation.

Tumorigenesis is controlled by the immune system, and the role of HA in the immune system has been studied extensively. Of note, HA binds to TLR2 and TLR4, which play important roles in innate immunity (18). We examined several parameters of the immune system, focusing first on macrophage functions, given that HA has been shown to alter immune responses via TLR4 that binds to LPS (18). However, macrophage activation and the severity of sepsis induced by i.p. injected LPS were not changed in Stab2 KO mice or in mice treated with the anti-Stab2 mAb (Figs. S2*E* and S4*C*). Furthermore, levels of inflammatory cytokines in serum and populations of various immune cells were not affected (Fig. S4 *A* and *B*). Therefore, inhibition of Stab2 function does not appear to directly affect the immune system. It is known that HA's functions depend on its molecular size, which varies from a few kDa to a few MDa (16). In the present study, HA molecules in Stab2 KO serum were ~40 kDa in size (Fig. S1*J*). possibly explaining some of the discrepancy between our results and those of previous studies.

Tumor cells circulate through the bloodstream and penetrate preferable tissues. Given that the s.c. proliferation of melanoma cells in Stab2 KO mice was not altered (Fig. 2*C*), we examined the initial step of attachment to the lungs. Melanoma cells expressing luciferase were injected via the tail vein, and cells trapped in the lungs were detected based on luciferase activity after perfusion with PBS to remove nonadherent cells. At 6 h after the i.v. injection, the number of melanoma cells trapped in the lungs was decreased in both the Stab2 KO mice and the mice given anti-Stab2, indicating that tumor metastasis is prevented at the initial stage of tissue penetration in the absence of Stab2 function (Fig. 5 *A* and *B*). Because those mice had extremely high plasma HA levels, we considered that the attachment of melanoma cells to the lungs is enhanced by HA displayed on the surface of blood vessels in normal lungs, and that a high level of HA in plasma blocks this interaction. In fact, melanoma cells adhered to HA-coated plates and pulmonary ECs, and HA at high concentrations, similar to those in serum of Stab2 KO mice, inhibited the attachment (Fig. 5, Fig. S3*F*, and Movies S1 and S2). Although i.v. injected HA is rapidly removed from the circulation, we found that the i.v. injection of a very high dose of HA was able to maintain the plasma HA concentration at a high level for at least 10 h (Fig. 5*C*). After the circulating HA level increased, B16F10 cells were injected to evaluate their attachment to the lungs. Metastasis of B16F10 cells to the lungs was markedly suppressed under these conditions (Fig. 3*D*). These results strongly suggest that inhibition of Stab2 function prevents tumor metastasis by elevating the plasma HA level.

Previous studies found that forced expression of HAS increased tumor cell proliferation and metastasis, whereas inhibition of HAS prevented proliferation and metastasis (23, 24, 30). These experiments suggested that HA promotes tumor proliferation and metastasis, whereas our results indicate that HA prevents metastasis. The critical difference between the previous studies and the present study is that we focused on the circulating HA, whereas most of the previous studies investigated extracellular matrix and pericellular HA. Therefore, it seems that the function of HA can differ depending on location.

In conclusion, our Stab2 KO mice were viable and exhibited no overt defects, but had dramatically increased plasma HA levels. This indicates that Stab2 is dispensable for normal development and homeostasis, and that an extremely high level of plasma HA has no deleterious effect. The increase in circulating HA levels was inversely correlated with metastasis and inhibited the attachment of melanoma cells to the lungs. Moreover, the administration of an anti-Stab2 mAb also increased the plasma HA level and blocked the metastasis of not only mouse melanoma cells, but also human breast tumor cells with no side effects. Thus, functional inhibition of Stab2 may be a potential strategy to suppress tumor metastasis.

## Materials and Methods

A Stab2 KO mouse line was generated by conventional methods, as described in *SI Materials and Methods*, and backcrossed with C57BL/6 for at least six generations. Anti-mouse Stab2 mAb (#34-2) was generated in our laboratory (10). Serum HA levels were measured with an HA assay kit (Seikagaku Biobusiness) in accordance with the manufacturer's instructions. The cell internalization of FITC-HA into HSECs was performed as described previously (10). For FACS analysis, HSECs were incubated with indicated antibodies and FITC-HA, and labeled cells were analyzed with a FACSCalibur flow cytometer (BD Biosciences). B16F10 cells [$5 \times 10^5$ (Fig. 2) or $5 \times 10^4$ (Fig. 3)] were injected into the tail vein. At 14 d after injection, the lung surface nodules were counted. For imaging in vivo, $5 \times 10^5$ B16F10-luc-G5 cells were injected i.v. At 7 d after the injection, metastasis was analyzed with luciferase luminescence as described previously (31). MDA-MB-231-luc-D3H2LN cells ($4 \times 10^6$) were injected into the mammary gland of SCID mice, and metastasis was analyzed using the IVIS imaging system (31, 32). 4T1-LucNeo-1H cells ($5 \times 10^4$) were injected into a mammary fad pad of SCID mice. Rolling and/or tethering of B16 melanoma cells onto cultured pulmonary ECs was analyzed under flow conditions at 0.7 dynes/cm$^2$ with the VenaEC System (Cellix) using confocal microscopy (Nikon A1R). Before the experiments, B16 melanoma cells were stained by CellTracker Red CMTPX (Molecular Probes) and Hoechst 33342 (Molecular Probes). Pulmonary ECs were also stained with CellTracker Green CMFDA (Molecular Probes) and Hoechst 33342. More detailed information is provided in *SI Materials and Methods*.

**ACKNOWLEDGMENTS.** We thank Dr. T. Akiyama for providing the B16F10 cells and Drs. H. Saya, T. Itoh, and M. Tanaka for valuable discussions and a critical reading of the manuscript. We also thank M. Tajima, C. Yoshinaga, and X. Yingda for their excellent technical help. This work was supported in part by research grants from the Ministry of Education, Culture, Sports, Science and Technology (MEXT) of Japan and the Ministry of Health, Labor and Welfare (MHLW) of Japan (to A.M.); the Centers of Research Excellence in Science and Technology program (A.M); the A-STEP program of the Japan Science and Technology Agency (Y.H.) and Takeda Science Foundation (to A.M.); the Funding Program for Next Generation World-Leading Researchers (to S.N.); the Japan Society for the Promotion of Science through its Funding Program for World-Leading Innovative Research and Development on Science and Technology (FIRST Program) (R.N.); Research Fellowships from a Grant-in-Aid 22113008 for Scientific Research on Innovative Areas of Fluorescence Live Imaging from The Ministry of Education, Culture, Sports, Science, and Technology of Japan (to S.N.); Grants-in-Aid for Scientific Research (to R.N.), grants for Translational Systems Biology and Medicine Initiative (to S.N. and R.N.), and the global Centers of Excellence program from the MEXT of Japan (R.N.); Banyu Life Science Foundation International (S.N.); and a research grant from the National Institute of Biomedical Innovation (to R.N.).

1. Fraser JR, Alcorn D, Laurent TC, Robinson AD, Ryan GB (1985) Uptake of circulating hyaluronic acid by the rat liver: Cellular localization in situ. *Cell Tissue Res* 242: 505–510.
2. Schledzewski K, et al. (2011) Deficiency of liver sinusoidal scavenger receptors stabilin-1 and -2 in mice causes glomerulofibrotic nephropathy via impaired hepatic clearance of noxious blood factors. *J Clin Invest* 121:703–714.
3. Politz O, et al. (2002) Stabilin-1 and -2 constitute a novel family of fasciclin-like hyaluronan receptor homologues. *Biochem J* 362:155–164.
4. Adachi H, Tsujimoto M (2002) FEEL-1, a novel scavenger receptor with in vitro bacteria-binding and angiogenesis-modulating activities. *J Biol Chem* 277:34264–34270.
5. Hansen B, et al. (2005) Stabilin-1 and stabilin-2 are both directed into the early endocytic pathway in hepatic sinusoidal endothelium via interactions with clathrin/AP-2, independent of ligand binding. *Exp Cell Res* 303:160–173.
6. Kzhyshkowska J, et al. (2005) Phosphatidylinositide 3-kinase activity is required for stabilin-1–mediated endosomal transport of acLDL. *Immunobiology* 210:161–173.
7. Kzhyshkowska J, et al. (2008) Alternatively activated macrophages regulate extracellular levels of the hormone placental lactogen via receptor-mediated uptake and transcytosis. *J Immunol* 180:3028–3037.
8. Kzhyshkowska J, et al. (2006) Novel function of alternatively activated macrophages: Stabilin-1-mediated clearance of SPARC. *J Immunol* 176:5825–5832.
9. Salmi M, Koskinen K, Henttinen T, Elima K, Jalkanen S (2004) CLEVER-1 mediates lymphocyte transmigration through vascular and lymphatic endothelium. *Blood* 104: 3849–3857.
10. Nonaka H, Tanaka M, Suzuki K, Miyajima A (2007) Development of murine hepatic sinusoidal endothelial cells characterized by the expression of hyaluronan receptors. *Dev Dyn* 236:2258–2267.
11. Park SY, et al. (2008) Rapid cell corpse clearance by stabilin-2, a membrane phosphatidylserine receptor. *Cell Death Differ* 15:192–201.
12. Gustafson S, Björkman T (1997) Circulating hyaluronan, chondroitin sulphate and dextran sulphate bind to a liver receptor that does not recognize heparin. *Glycoconj J* 14:561–568.
13. Harris EN, Weigel PH (2008) The ligand-binding profile of HARE: Hyaluronan and chondroitin sulfates A, C, and D bind to overlapping sites distinct from the sites for heparin, acetylated low-density lipoprotein, dermatan sulfate and CS-E. *Glycobiology* 18:638–648.
14. Kogan G, Soltés L, Stern R, Gemeiner P (2007) Hyaluronic acid: A natural biopolymer with a broad range of biomedical and industrial applications. *Biotechnol Lett* 29: 17–25.
15. Fraser JR, Laurent TC, Laurent UB (1997) Hyaluronan: Its nature, distribution, functions and turnover. *J Intern Med* 242:27–33.
16. Stern R, Asari AA, Sugahara KN (2006) Hyaluronan fragments: An information-rich system. *Eur J Cell Biol* 85:699–715.
17. Almond A (2007) Hyaluronan. *Cell Mol Life Sci* 64:1591–1596.
18. Jiang D, et al. (2005) Regulation of lung injury and repair by Toll-like receptors and hyaluronan. *Nat Med* 11:1173–1179.
19. DeGrendele HC, Estess P, Siegelman MH (1997) Requirement for CD44 in activated T cell extravasation into an inflammatory site. *Science* 278:672–675.
20. Zöller M (2011) CD44: Can a cancer-initiating cell profit from an abundantly expressed molecule? *Nat Rev Cancer* 11:254–267.
21. Banerji S, et al. (1999) LYVE-1, a new homologue of the CD44 glycoprotein, is a lymph-specific receptor for hyaluronan. *J Cell Biol* 144:789–801.
22. Kim S, et al. (2009) Carcinoma-produced factors activate myeloid cells through TLR2 to stimulate metastasis. *Nature* 457:102–106.
23. Sironen RK, et al. (2011) Hyaluronan in human malignancies. *Exp Cell Res* 317: 383–391.
24. Toole BP (2004) Hyaluronan: From extracellular glue to pericellular cue. *Nat Rev Cancer* 4:528–539.
25. Twarock S, et al. (2011) Inhibition of oesophageal squamous cell carcinoma progression by in vivo targeting of hyaluronan synthesis. *Mol Cancer* 10:30.
26. Kudo D, et al. (2004) Effect of a hyaluronan synthase suppressor, 4-methylumbelliferone, on B16F-10 melanoma cell adhesion and locomotion. *Biochem Biophys Res Commun* 321:783–787.
27. Zhou B, Weigel JA, Fauss L, Weigel PH (2000) Identification of the hyaluronan receptor for endocytosis (HARE). *J Biol Chem* 275:37733–37741.
28. Harris EN, Weigel JA, Weigel PH (2008) The human hyaluronan receptor for endocytosis (HARE/Stab2) is a systemic clearance receptor for heparin. *J Biol Chem* 283: 21453–21461.
29. Gale NW, et al. (2007) Normal lymphatic development and function in mice deficient for the lymphatic hyaluronan receptor LYVE-1. *Mol Cell Biol* 27:595–604.
30. Yoshihara S, et al. (2005) A hyaluronan synthase suppressor, 4-methylumbelliferone, inhibits liver metastasis of melanoma cells. *FEBS Lett* 579:2722–2726.
31. Takeshita F, et al. (2005) Efficient delivery of small interfering RNA to bone-metastatic tumors by using atelocollagen in vivo. *Proc Natl Acad Sci USA* 102:12177–12182.
32. Jenkins DE, Hornig YS, Oei Y, Dusich J, Purchio T (2005) Bioluminescent human breast cancer cell lines that permit rapid and sensitive in vivo detection of mammary tumors and multiple metastases in immune deficient mice. *Breast Cancer Res* 7:R444–R454.

Gene Therapy (2012) 19, 34–48

www.nature.com/gt

ORIGINAL ARTICLE

# *In vivo* delivery of *interferon-α* gene enhances tumor immunity and suppresses immunotolerance in reconstituted lymphopenic hosts

K Narumi[1,4], T Udagawa[1], A Kondoh[1], A Kobayashi[1], H Hara[1], Y Ikarashi[1], S Ohnami[2], F Takeshita[3], T Ochiya[3], T Okada[4], M Yamagishi[4], T Yoshida[2] and K Aoki[1]

T cells recognize tumor-associated antigens under the condition of lymphopenia-induced homeostatic proliferation (HP); however, HP-driven antitumor responses gradually decay in association with tumor growth. Type I interferon (IFN) has important roles in regulating the innate and adaptive immune system. In this study we examined whether a tumor-specific immune response induced by IFN-α could enhance and sustain HP-induced antitumor immunity. An intratumoral *IFN-α* gene transfer resulted in marked tumor suppression when administered in the early period of syngeneic hematopoietic stem cell transplantation (synHSCT), and was evident even in distant tumors that were not transduced with the IFN-α vector. The intratumoral delivery of the *IFN-α* gene promoted the maturation of CD11c$^+$ cells in the tumors and effectively augmented the antigen-presentation capacity of the cells. An analysis of the cytokine profile showed that the CD11c$^+$ cells in the treated tumors secreted a large amount of immune-stimulatory cytokines including interleukin (IL)-6. The CD11c$^+$ cells rescued effector T-cell proliferation from regulatory T-cell-mediated suppression, and IL-6 may have a dominant role in this phenomenon. The intratumoral *IFN-α* gene transfer creates an environment strongly supporting the enhancement of antitumor immunity in reconstituted lymphopenic recipients through the induction of tumor-specific immunity and suppression of immunotolerance.
Gene Therapy (2012) **19**, 34–48; doi:10.1038/gt.2011.73; published online 26 May 2011

**Keywords:** IFN-α; gene transfer; hematopoietic stem cell transplantation; IL-6; regulatory T cells

## INTRODUCTION

The development of effective cancer immunotherapy is often difficult because cancer generates an immunotolerant microenvironment against the host immune system.[1] The central objective of cancer immunotherapy is to induce and sustain a tumor-specific immune response; that is, an *in vivo* generation of a large number of highly reactive antitumor lymphocytes that are not restrained by cancer-induced tolerance mechanisms.

It is known that lymphopenia is followed by spontaneous expansion of the remaining T cells in the periphery to restore the original T-cell pool size and maintain homeostasis.[2] Lymphopenia-induced homeostatic proliferation (HP) of T cells following autologous hematopoietic stem cell transplantation (HSCT) is driven by the recognition of self-antigens, and there is an opportunity to skew the T-cell repertoire during the T-cell recovery by engaging tumor-associated antigens (TAAs), leading to a break in tolerance developed by tumors.[2] In fact, a variety of animal tumor models showed that lymphopenic conditions are able to create an environment to mount an efficient antitumor immunity through an HP-induced expansion of T cells.[3–6] However, integration of other immunotherapeutic strategies is necessary to successfully eradicate pre-existing malignant tumors, because HP-driven antitumor responses decay gradually, as they are vulnerable to a development of tolerance.[5,6]

The interferon (IFN)-α protein is a pleiotropic cytokine regulating anti-proliferation, induction of cell death, anti-angiogenesis and immunomodulation, and has been used for treatment in a variety of cancers such as chronic myeloid leukemia, melanoma and renal cancer.[7,8] Although IFN-α was long thought to function mainly by suppressing tumor cell proliferation *in vivo*, more recently it has been established that type I IFNs have important roles in regulating the innate and adaptive arms of the immune system: upregulation of major histocompatibility complex class I gene, promotion of the priming and survival of T cells, enhancement of humoral immunity, increase of the cytotoxic activity of natural killer (NK) cells and CD8$^+$ T cells and activation of dendritic cells (DCs).[9,10] We also reported that in addition to the direct cytotoxicity in the injected site, intratumoral *IFN-α* gene transfer elicits a systemic tumor-specific immunity in several animal models.[11,12] Furthermore, our data showed that, because of the effective induction of antitumor immunity and the lower toxicity, an intratumoral route of the IFN vector is superior to an intravenous administration.[13]

In this study, we examined whether HP-induced antitumor activity can be enhanced by IFN-α gene transfer during a physiological

[1]Division of Gene and Immune Medicine, National Cancer Center Research Institute, Tokyo, Japan; [2]Division of Genetics, National Cancer Center Research Institute, Tokyo, Japan; [3]Division of Molecular and Cellular Medicine, National Cancer Center Research Institute, Tokyo, Japan and [4]Department of Internal Medicine, Kanazawa University Graduate School of Medical Science, Ishikawa, Japan
Correspondence: Dr K Aoki, Section for Studies on Host-Immune Response, National Cancer Center Research Institute, 5-1-1 Tsukiji, Chuo-ku, Tokyo 104-0045, Japan.
E-mail: kaoki@ncc.go.jp
Received 25 September 2010; revised 4 April 2011; accepted 19 April 2011; published online 26 May 2011

immune reconstitution, and investigated mechanisms of the enhancement. From the viewpoint of IFN-α immune therapy also, an autologous HSCT following a preconditioning is expected to introduce a fresh immune system, in which tolerance to tumor cells is not yet induced, and may present a unique opportunity for IFN-α to augment efficacy of the immune therapy.

## RESULTS

### Adenovirus-mediated *IFN-α* gene transfer induces significant antitumor effect with synHSCT

To examine whether HP of T cells could induce antitumor immunity in lymphopenic hosts, BALB/c mice were injected subcutaneously with CT26 colon cancer cells shortly after lethal (9 Gy) irradiation, and then bone marrow and T cells were infused into the mice. Tumor growth was significantly suppressed in the syngeneic HSCT (synHSCT) recipients (Figure 1a) as previously reported.[6] HSCT with immunodeficient mice did not show the tumor growth suppression as compared with non-transplanted mice (data not shown), indicating that the antitumor effect is not mediated by a nonspecific effect of irradiation or lymphocyte infusion. Then, to examine whether a combination of intratumoral *IFN-α* gene transfer enhances the antitumor effect of synHSCT, $5\times10^6$ PFU (plaque forming unit) of Ad-mIFN was injected once into the tumor at 5 days after the CT26 inoculation. To detect a synergistic effect, we used a low dose ($5\times10^6$ PFU) of Ad-mIFN in this experiment, although the antitumor effect of intratumoral Ad-mIFN injection is dose-dependent, and a strong antitumor effect is induced by a high dose ($5–10\times10^7$ PFU) of Ad-mIFN alone.[12,13] Although the low dose of Ad-mIFN alone suppressed tumor growth only slightly in naïve mice as expected, a significant growth suppression was observed in the synHSCT recipients compared with the injection of a control Ad-AP (Figure 1b).

### Injection of IFN-α-expressing plasmid suppresses tumor growth in synHSCT recipients

We observed a significant growth suppression of colon cancer in a lymphopenic host by an injection of a low dose of Ad-mIFN (Figure 1b). Although the *in vivo* gene transduction efficiency of the plasmid vector is lower than that of the virus vector, the lipofection/

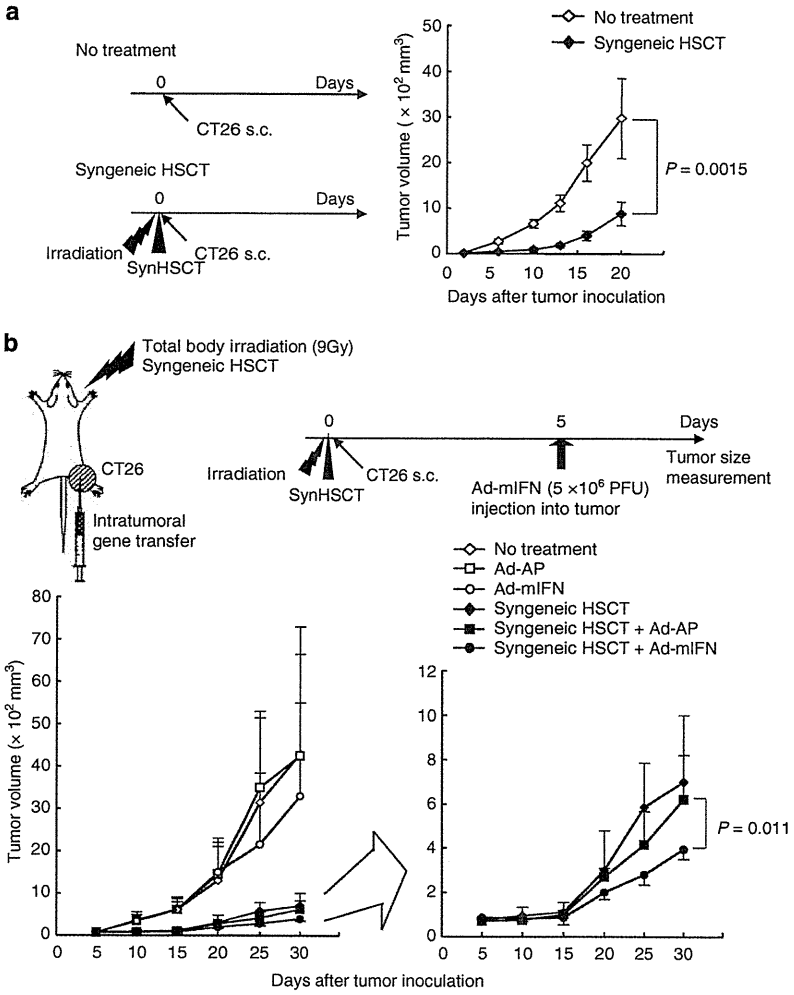


**Figure 1** Adenovirus-mediated *IFN-α* gene transfer enhances antitumor effect in synHSCT recipients. (**a**) Growth suppression of subcutaneous tumors in the synHSCT mice. The mice received a lethal dose (9 Gy) of irradiation, followed by a transfusion of bone marrow and splenic T cells, and then CT26 cells were inoculated into right legs. As a control, CT26 cells were inoculated in non-irradiated mice ($n$=7). (**b**) A combination of syngeneic HSCT and IFN-α adenovirus injection. When CT26 subcutaneous tumors were established, $5\times10^6$ PFU of Ad-mIFN or control vector (Ad-AP) were injected once into the tumors ($n$=6–8). The experiments were repeated two times.

polyfection of the plasmid vector has an excellent safety profile.[14] Therefore, we examined whether tumor growth suppression would be observed by an injection of an IFN-α-expressing plasmid (pIFN-α). First, we confirmed that CT26 and Renca cells transfected with the pIFN-α produced significant amounts of IFN-α protein in the culture medium (Figure 2a), and showed growth suppression *in vitro* (Figure 2b). In CT26 tumor-bearing BALB/c mice, the injection of pIFN-α complexed with cationic liposome (DMRIE-DOPE) expressed IFN-α in the tumors in a dose-dependent manner, and an IFN-α concentration by the injections of pIFN-α (30 μg, three times) was comparable with that of Ad-mIFN ($5\times10^6$ PFU, once) (Figure 2c). The plasmid-mediated IFN-α expression continued for more than 10 days after gene transfer and returned to a control level at 14 days after gene transfer (Figure 2d).

Then, to examine the *in vivo* antitumor effect of a plasmid-mediated *IFN-α* gene transfer, a pIFN-α/liposome complex was injected into the CT26 subcutaneous tumors at 7 days after the transplantation. The injection of pIFN-α slightly suppressed tumor growth compared with the non-injected control group, whereas the tumor-suppressive effect by the injection of pIFN-α was significantly enhanced in the lymphopenic mice that received synHSCT (Figure 2e). The results suggested that an *in vivo* injection of pIFN-α induced antitumor immunity in lymphopenic hosts as effectively as the Ad-mIFN. Regarding the timing of intratumoral *IFN-α* gene transfer, the injection of pIFN-α at 8 weeks after transplantation did not enhance the antitumor immunity, whereas a substantial antitumor effect was observed by *IFN-α* gene transfer in the earlier period (2–6 weeks) after the transplantation (Figure 2f), suggesting that intratumoral *IFN-α* gene transfer during immune reconstitution can induce a synergistic antitumor effect. In the mice treated with *IFN-α* gene transfer at 6 weeks after HSCT, tumor growth suppression was still recognized ($P=0.016$) at day 42 and the survival of the treated mice was significantly prolonged as compared with the injection of the control plasmid (Figure 2g). All treated mice looked healthy during the course of the experiments, and the blood chemistry (albumin, alanine transaminase, total bilirubin, alkaline phosphatase, blood urea nitrogen, creatinine) showed no abnormal values in the treated mice at 5 weeks after the HSCT.

### Intratumoral *IFN-α* gene transfer increases tumor-infiltrating lymphocytes after synHSCT

It is known that a large number of tumor-infiltrating lymphocytes (TILs) results in a better prognosis for cancer patients.[15] To examine whether an increase of TILs in treated tumors is related to tumor growth suppression, immunohistochemical staining of CD4 and CD8-positive cells was performed at 1–4 weeks after synHSCT. In this experiment, CT26 cells were inoculated on legs at 1 week before synHSCT, and the number of $CD4^+$ and $CD8^+$ T cells infiltrated into the tumors was examined at the day of synHSCT to evaluate how the number of immune cells increases in the tumors by the combination therapy as compared with the pre-treatment status. In this established tumor model also, a significant antitumor effect was recognized in the synHSCT mice with the *IFN-α* gene transfer (Figure 3a).

The numbers of $CD4^+$ and $CD8^+$ cells gradually diminished in the non-treated tumors, whereas the TILs increased in the tumors of synHSCT mice. Intratumoral *IFN-α* gene transfer further increased the numbers of TILs significantly in synHSCT recipients at 4 weeks (Figure 3b), suggesting that intratumoral *IFN-α* gene transfer enhances and prolongs HP-induced antitumor immunity after synHSCT.

Then, to examine the cytotoxic activity of TILs, $CD8^+$ T cells were isolated from tumors in the treated mice. The flow cytometry showed that the expression of perforin on $CD8^+$ TILs was significantly enhanced in the synHSCT alone group and in the combination therapy-treated group, suggesting that synHSCT creates an environment to enhance the killing activity of TILs in the tumors (Figure 3c).

### Tumor-specific lymphocytes are activated by intratumoral *IFN-α* gene transfer in synHSCT recipients

To examine the immune reaction to intratumoral *IFN-α* gene transfer in synHSCT recipients, splenocytes were extracted from the treated mice and cultured with CT26 cells. An enzyme-linked immunosorbent spot assay showed that the average number of IFN-γ-producing splenocytes in response to CT26 cells was slightly increased in the synHSCT alone group, whereas a combination of synHSCT and intratumoral *IFN-α* gene transfer further increased the IFN-γ-positive spots (Figure 4a, left panel). The numbers of the spots in splenocytes co-cultured with syngeneic lymphocytes were not changed in the treated groups (Figure 4a, right panel). To analyze the subset of activated lymphocytes, the frequency of tumor-reactive immune cells was determined by intracellular cytokine staining and flow cytometry. The percentage of $CD4^+$ and $CD8^+$ T cells stimulated to produce IFN-γ in response to CT26 cells increased significantly in the mice treated by a combination of synHSCT and intratumoral *IFN-α* gene transfer, and there was also an increase in the percentage of IFN-γ-positive NK cells (Figure 4b). The results indicated that the numbers of tumor-reactive lymphocytes were increased synergistically by a combination therapy.

An *in vitro* cytotoxic assay showed that the splenocytes derived from the synHSCT mice recognized and lysed CT26 cells, and *IFN-α* gene transfer enhanced the cytolysis to CT26 cells (Figure 4c, left panel). To

**Figure 2** Plasmid vector-mediated *IFN-α* gene transfer induces a significant antitumor effect in synHSCT recipients. (**a**) *In vitro* IFN-α concentration in the medium of cancer cells transfected with pIFN-α. CT26 or Renca cells were transfected with pIFN-α, and 48 h later, IFN-α concentration in the culture medium was measured by enzyme-linked immunosorbent assay (ELISA; Immunotech, Marseille Cedex, France). pEGFP was used as a control. (**b**) *In vitro* cytotoxicity of pIFN-α transfection. The cell growth was determined by an *in vitro* cell proliferation assay at 5 days after transfection. The data are expressed as relative cell growth ($OD_{450}$ of indicated cells/$OD_{450}$ of untreated cells). Reagent; Lipofectamine 2000. (**c**) *In vivo* IFN-α concentration in the tumors transfected with pIFN-α. Various amounts (10–30 μg) of pIFN-α complexed with liposome were injected three times into the CT26 tumors at 7, 9 and 11 days after the tumor inoculation. Ad-mIFN ($5\times10^6$ PFU) was injected once into the tumors at day 9. Tumors were collected at day 12, and the IFN-α concentration was measured by ELISA ($n=4$). (**d**) Time course of IFN-α expression in the tumors. The IFN-α levels were measured in the subcutaneous tumors during 14 days after intratumoral injection of pIFN-α (30 μg)/liposome complex at days 7, 9 and 11 ($n=4$–5). The statistical difference between IFN-α concentration in the indicated days and at day 7 is presented. (**e**) A combination of syngeneic HSCT and intratumoral *IFN-α* gene transfer caused marked tumor growth suppression. The pIFN-α (30 μg)/liposome complex was injected into the CT26 tumors at 7, 9 and 11 days after the tumor inoculation in the synHSCT mice ($n=7$). The experiments were repeated two times. (**f**) Intratumoral *IFN-α* gene transfer during an early phase of immune reconstitution enhances the antitumor effects. Syngeneic HSCTs to the BALB/c mice were staggered at intervals of 2 weeks, followed by a subcutaneous injection of CT26 cells and intratumoral *IFN-α* gene transfer at days 7, 9 and 11 ($n=6$–8). (**g**) Intratumoral *IFN-α* gene transfer significantly extends the survival of synHSCT mice ($n=7$). The pIFN-α/liposome complex was injected into the CT26 tumors at 6 weeks after the HSCT, and survival of the mice was compared with the mice injected with a control plasmid ($n=7$).

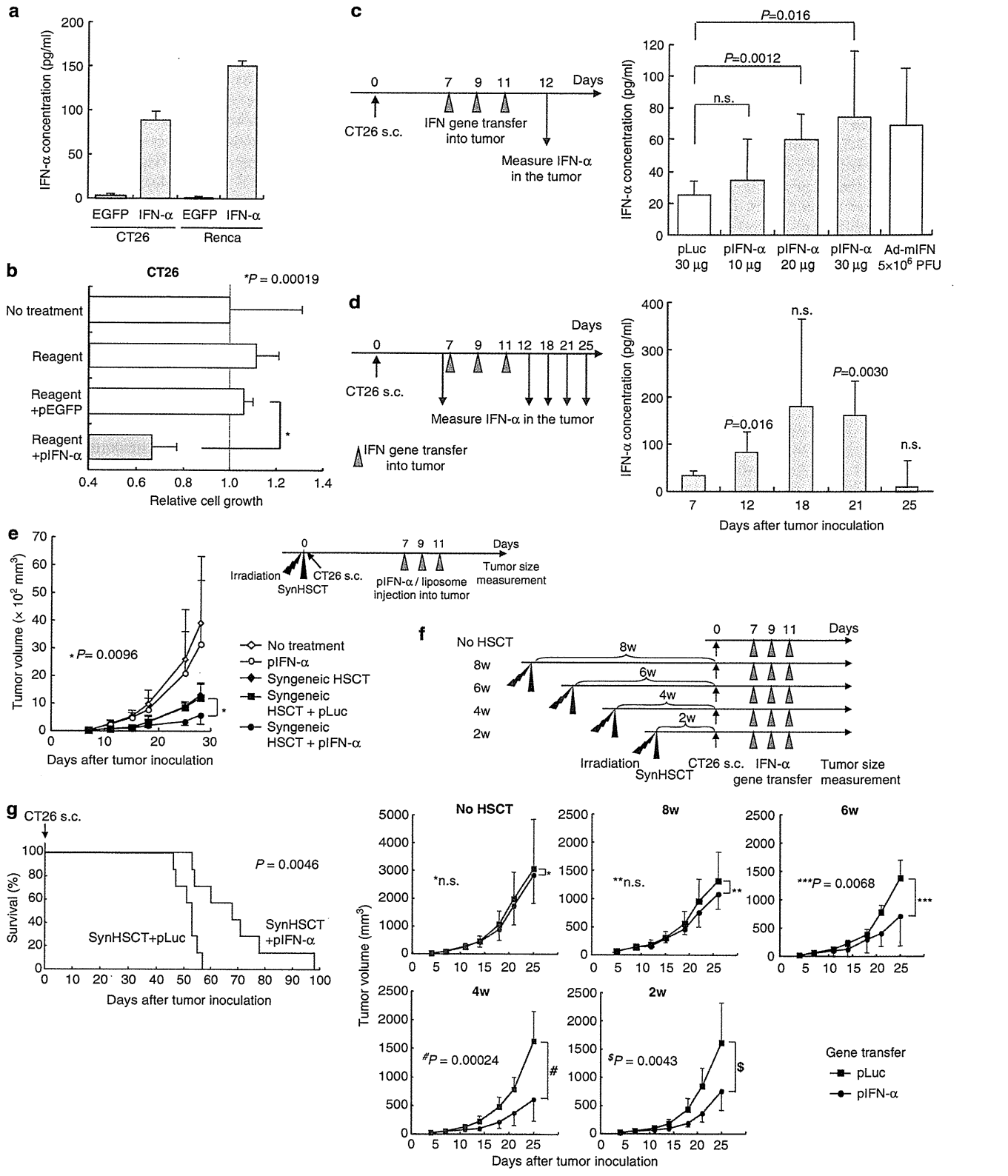
a
IFN-α concentration (pg/ml)
200
150
100
50
0
EGFP IFN-α EGFP IFN-α
CT26
Renca
b
CT26
*P = 0.00019
No treatment
Reagent
Reagent +pEGFP
Reagent +pIFN-α
0.4 0.6 0.8 1.0 1.2 1.4
Relative cell growth
c
0 7 9 11 12 Days
CT26 s.c.
IFN gene transfer into tumor
Measure IFN-α in the tumor
P=0.016
P=0.0012
n.s.
IFN-α concentration (pg/ml)
120
100
80
60
40
20
0
pLuc 30 μg
pIFN-α 10 μg
pIFN-α 20 μg
pIFN-α 30 μg
Ad-mIFN 5×10^6 PFU
d
0 7 9 11 12 18 21 25 Days
CT26 s.c.
Measure IFN-α in the tumor
IFN gene transfer into tumor
IFN-α concentration (pg/ml)
400
300
200
100
0
n.s.
P=0.0030
P=0.016
n.s.
7 12 18 21 25
Days after tumor inoculation
e
Tumor volume (× 10^2 mm^3)
70
60
50
40
30
20
10
0
*P= 0.0096
0 10 20 30
Days after tumor inoculation
0 7 9 11 Days
Irradiation
CT26 s.c.
SynHSCT
pIFN-α / liposome injection into tumor
Tumor size measurement
No treatment
pIFN-α
Syngeneic HSCT
Syngeneic HSCT + pLuc
Syngeneic HSCT + pIFN-α
f
No HSCT
8w
6w
4w
2w
0 7 9 11 Days
Irradiation
SynHSCT
CT26 s.c.
IFN-α gene transfer
Tumor size measurement
g
CT26 s.c.
Survival (%)
100
80
60
40
20
0
P = 0.0046
SynHSCT+pLuc
SynHSCT +pIFN-α
0 10 20 30 40 50 60 70 80 90 100
Days after tumor inoculation
Tumor volume (mm^3)
No HSCT
*n.s.
8w
**n.s.
6w
***P = 0.0068
4w
#P = 0.00024
2w
$P = 0.0043
0 5 10 15 20 25
Days after tumor inoculation
Gene transfer
pLuc
pIFN-α

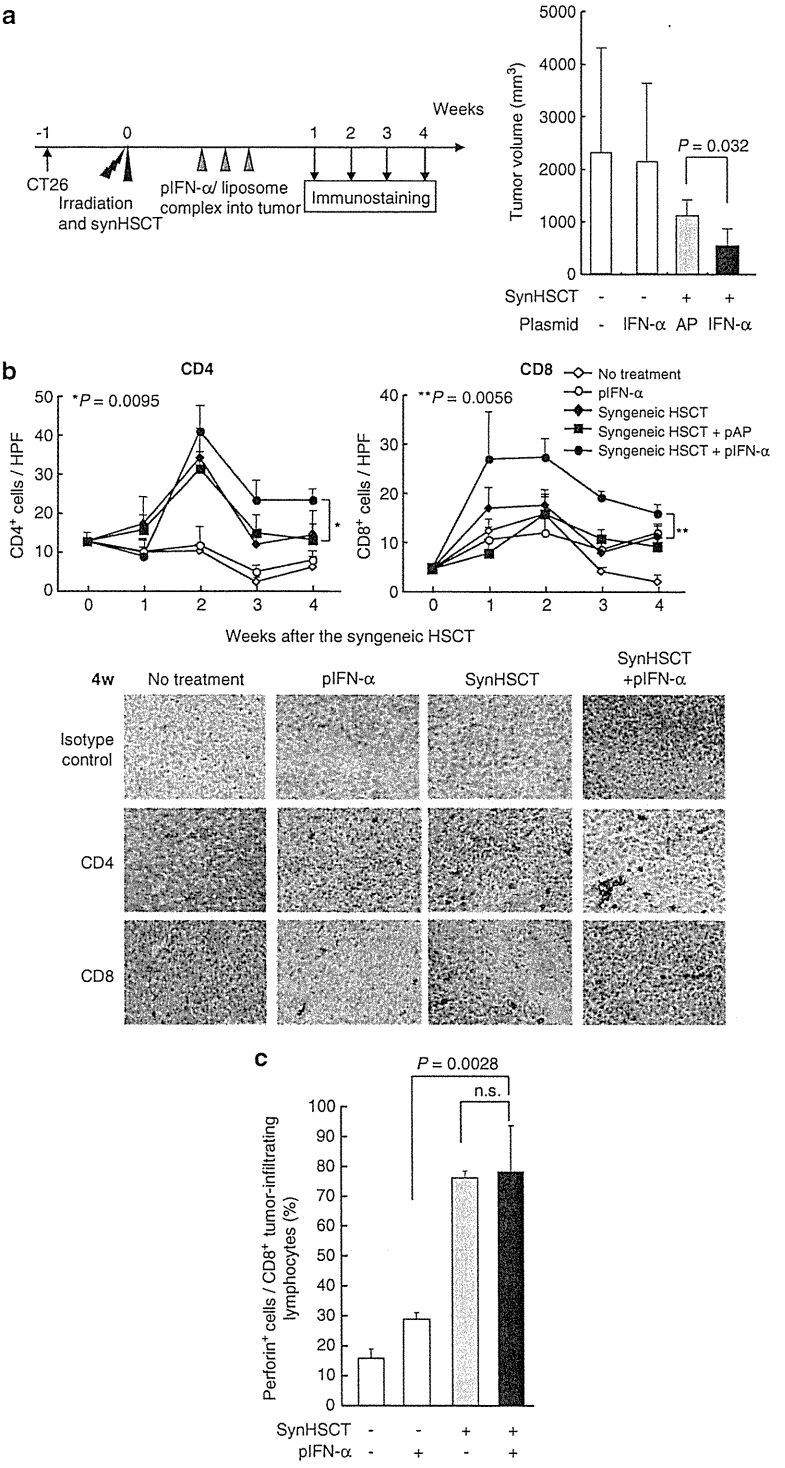


**Figure 3** Immunostaining of treated tumors. (**a**) Antitumor effect of *IFN-α* gene transfer for established tumors in the synHSCT recipient mice. CT26 cells were inoculated on the right legs of BALB/c mice at 1 week before the synHSCT, and the pIFN-α/liposome complex was injected into CT26 tumors for three times. The tumor volumes at 3 weeks after the *IFN-α* gene transfer are presented. (**b**) Infiltration of immune cells in the tumors. The subcutaneous tumors were resected at the indicated days ($n$=3), and stained with CD4 and CD8 antibodies. The $CD4^+$ (upper left) and $CD8^+$ cells (upper right) were counted by microscopy in five high-power fields (×400). Representative photographs of stained cells at 4 weeks after the gene transfer are presented in the lower panel (×400). (**c**) Expression of perforin on $CD8^+$ tumor-infiltrating lymphocytes. The $CD8^+$ T cells were isolated from the tumors using mouse CD8 MicroBeads and AutoMACS magnetic sorter (Miltenyi Biotec, Bergisch Gladbach, Germany). The flow cytometry of perforin (eBioOMAK-D; eBioscience, San Diego, CA, USA) was performed on the $CD8^+$ TILs ($n$=3). The frequency of $perforin^+$ cells per $CD8^+$ cells is presented.

show the major histocompatibility complex class I-restriction of cytotoxicity, lymphocytes were pre-incubated with the anti-CD4 or anti-CD8 antibodies before the cytolysis for CT26 cells. The addition of anti-CD8 antibody markedly inhibited the cell lysis (Figure 4c, right panel).

To explore what kind of lymphocytes contribute to antitumor immunity *in vivo*, the mice were treated with anti-CD4, anti-CD8 and anti-asialo GM1 antibodies intraperitoneally to deplete $CD4^+$ T cells, $CD8^+$ T cells and NK cells, respectively. Depletion of all of the three populations canceled antitumor effect almost completely. Depletion of each $CD4^+$ T-cell, $CD8^+$ T-cell or NK cell showed some growth advantages but still resulted in significant tumor growth inhibition and, in particular, $CD8^+$ T cells appeared to contribute more strongly than $CD4^+$ T and NK cells (Figure 4d).

### Intratumoral *IFN-α* gene transfer causes growth suppression in not only treated but also distant tumors

To evaluate the therapeutic efficacy of *IFN-α* gene transfer against tumors at distant sites in synHSCT recipients, the mice were inoculated with CT26 cells on both legs and Renca cells on the back, and an IFN-α plasmid/liposome complex was injected into the CT26 tumor on the right leg. The *IFN-α* gene transfer significantly suppressed the growth of not only the right leg CT26 tumors but also the left CT26 tumors that were not transfected with the *IFN-α* gene, whereas the growth of Renca tumors on the back was not influenced by the *IFN-α* gene transfer into the CT26 tumors (Figure 5a). When we exchanged CT26 and Renca cells, the antitumor effect was *vice versa* (Figure 5b). The results indicated that intratumoral *IFN-α* gene transfer enhances a vector-injected-tumor specific immunity systemically in the synHSCT recipients.

Liver metastasis is one of the most frequent causes of mortality in patients with gastrointestinal cancer such as colorectal cancer. As another model of distant metastasis, CT26-Luc cells were injected beneath the splenic capsule to generate liver metastasis, and CT26 cells were inoculated into the right leg. Intratumoral *IFN-α* gene transfer suppressed tumor growth of subcutaneous tumors on the legs (Figure 5c, upper left panel) as observed in Figure 2e, and the growth of abdominal tumors was also markedly suppressed, which were evaluated by photon counts on the IVIS imaging system (IVIS; Xenogen, Alameda, CA, USA), in the synHSCT mice (Figure 5c, upper right and lower panels). Twenty-one days after tumor inoculation, the mice were killed and the livers were examined by the IVIS imaging. Livers from non-treated mice showed many photon-positive spots, whereas livers from the mice treated by a combination therapy revealed a fewer number of photon-positive spots (Figure 5d, upper panel), which was confirmed by photon counts in those livers (Figure 5d, lower panel). These results indicated that a combination therapy is effective for preventing and regressing liver metastases.

### A combination therapy enhances maturation of $CD11c^+$cells and their antigen presentation

To verify whether the intratumoral *IFN-α* gene expression promotes the maturation of DCs in the tumor, we isolated $CD11c^+$ cells from the regional lymph nodes of treated tumors. Flow cytometry showed that expressions of CD40, CD80, CD83 and CD86 were clearly upregulated by the *IFN-α* gene transfer (data not shown and see Narumi *et al.*[13]). Then, the expression of CD83 was examined in the $CD11c^+$ cells isolated from tumors. The frequency of $CD83^+$ cells was increased in IFN/HSCT-$CD11c^+$ cells compared with those in IFN-$CD11c^+$ and HSCT-$CD11c^+$ cells (Figure 6a, left panel), suggesting that IFN-α expression results in the maturation of $CD11c^+$ cells. Then, to examine the antigen-presentation capacity of the $CD11c^+$ cells in the tumors, the lymphocytes isolated from naïve mice were co-cultured with the $CD11c^+$ cells and mitomycin C-treated CT26 cells for 3 days. An enzyme-linked immunosorbent spot assay showed that the IFN/HSCT-$CD11c^+$ cells increased the number of IFN-γ-positive lymphocytes in response to CT26 cells (Figure 6a, middle panel). The production of IFN-γ from the $CD11c^+$ cells *per se* was minimal. Lymphocytes under HP are considered to be primed to TAAs. When lymphocytes isolated from tumor-bearing synHSCT mice were co-cultured with the $CD11c^+$ cells and mitomycin C-treated CT26 cells, the stimulation by IFN/HSCT-$CD11c^+$ cells resulted in a higher number of IFN-γ-secreting lymphocytes than those of IFN-$CD11c^+$ and HSCT-$CD11c^+$cells (Figure 6a, right panel). The results indicated that the antigen-presentation by $CD11c^+$ cells was enhanced by the IFN-α expression in the tumors in synHSCT mice.

### $CD11c^+$cells treated by a combination therapy suppresses the activity of regulatory T cells

To analyze the cytokine expression profile of the $CD11c^+$ cells, we collected $CD11c^+$ cells from the treated tumor at 2 weeks after *IFN-α* gene transfer, cultured the cells *in vitro* for 48 h and measured the expression of various cytokines in the medium. The IFN/HSCT-$CD11c^+$ cells produced a large amount of immune-stimulatory cytokines such as interleukin (IL)-1β, IL-6 and IL-12 (Figure 6b), which may enhance the proliferation and activation of lymphocytes in the treated mice. Among the immunosuppressive cytokines (IL-4, IL-10 and transforming growth factor-β), IL-10 production is increased in IFN/HSCT-$CD11c^+$ cells. The enhanced IL-12 production might promote the production of IL-10 in some population of the $CD11c^+$ cells as a negative feedback mechanism.[16] However, the large amount of immune-stimulatory cytokines may overcome the suppressive effect of IL-10 in the tumors treated with the combination therapy.

IL-6 is of particular interest, because, when released from DCs, it is critical for overcoming Tregs-mediated immune suppression.[17] When the $CD11c^+$ cells isolated from the spleen of synHSCT and non-HSCT mice were cultured in the medium containing IFN-α protein, the cells produced IL-6 in a dose-response manner (Figure 7a). To examine whether the $CD11c^+$ cells inhibit the suppressive activity of Tregs, $CD11c^+$ cells were isolated from regional lymph nodes and co-cultured with $CD4^+CD25^-$ T cells (target) and $CD4^+CD25^+$ Tregs in mouse anti-CD3 T-cell activation plates. When Tregs were co-cultured with the control $CD11c^+$ cells isolated from non-treated mice, Tregs effectively suppressed the proliferation of target T cells. The co-culture with IFN/HSCT-$CD11c^+$ cells canceled the suppressive activity of Tregs for effector T cells (Figure 7b). The supernatant of IFN/HSCT-$CD11c^+$ cells also inhibited the suppressive activity of Tregs, and the addition of anti-IL-6 antibody in the medium restored the activity of Tregs, indicating that the critical factor of $CD11c^+$ cell-mediated inhibition of Tregs is IL-6, produced from activated $CD11c^+$ cells (Figure 7c).

Then, to examine the *in vivo* effect of intratumoral IFN-α expression on Tregs, we collected lymphocytes from treated tumors in synHSCT mice. Flow cytometry showed that intratumoral *IFN-α* gene transfer decreased the ratio of $Foxp3^+$ cells per $CD4^+$ T cells in the tumors of synHSCT mice, whereas the ratio of $Foxp3^+$ cells in the spleen was same as that in the non-treated mice (Figure 7d). The results suggested that IL-6 produced from $CD11c^+$ cells decreases the ratio of Tregs in the treated tumors. IFN-α expression may result in the extensive infiltration of T cells into the tumors of synHSCT mice (Figure 3b), and the number of $Foxp3^+$ cells also might increase in the

tumors. However, as the antitumor immune response is based on the balance between the effector and regulatory sides of immune cells; the decrease of Treg ratio (Figure 7d) and inhibition of Treg activity (Figure 7b) may lead to a strong antitumor immunity.

## DISCUSSION

In this study, we showed that an intratumoral *IFN-α* gene transfer significantly enhances a systemic tumor-specific immunity in the synHSCT recipients. The precise mechanism for the enhancement is

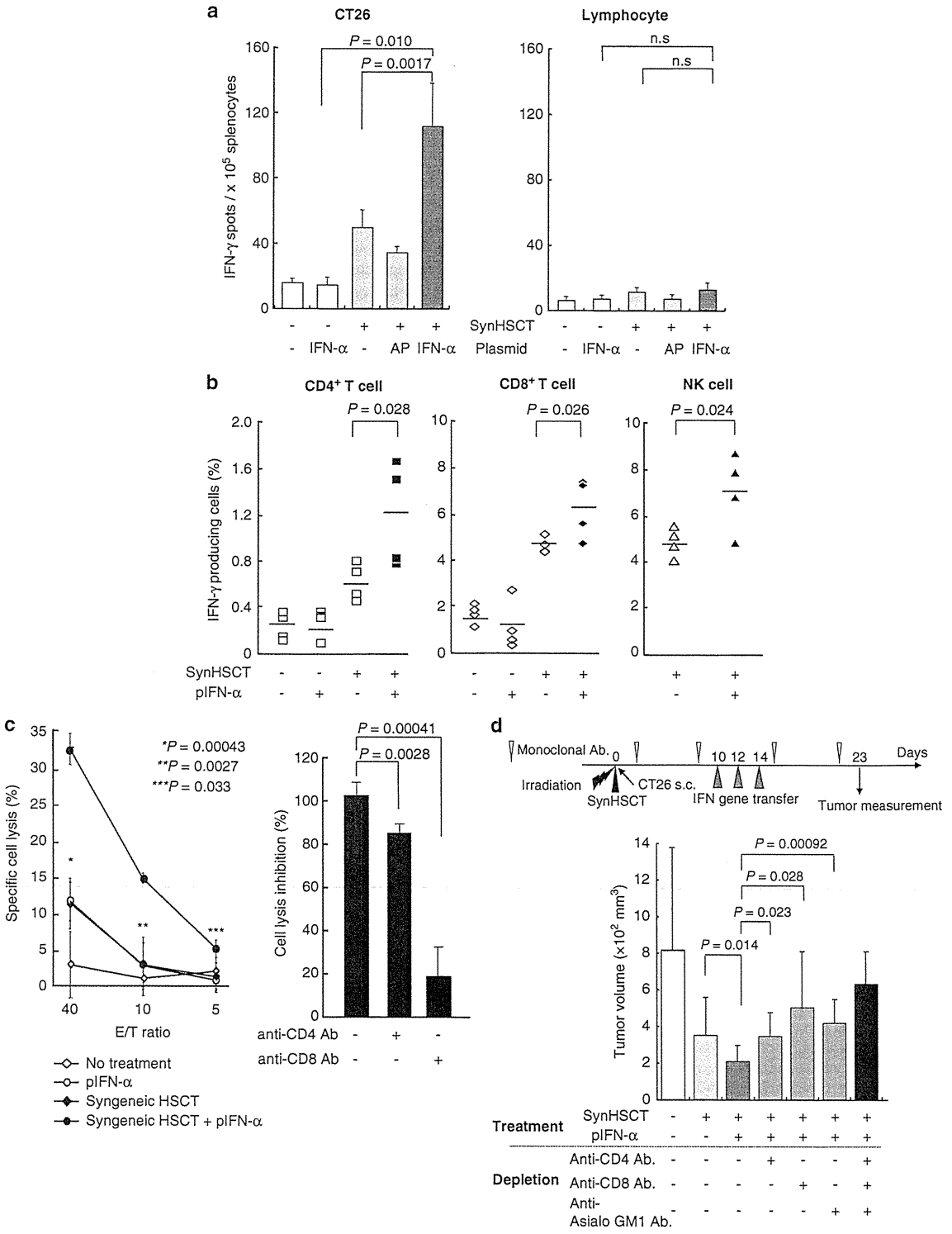

not completely understood, but it should include an effective stimulation of DCs by the expression of IFN-α in the tumors in synHSCT recipients, because (1) intratumoral expression of IFN-α effectively induces cell death of cancer cells and exposes TAAs in large quantity to DCs ($CD11c^+$ cells);[12] (2) IFN-α promotes maturation of $CD11c^+$ cells, which facilitates the presentation of TAAs on $CD11c^+$ cells (Figure 6a); (3) $CD11c^+$ cells in the tumors transduced with the *IFN-α* gene produce a large quantity of immune-stimulatory cytokines such as IL-12 (Figure 6b); (4) the $CD11c^+$ cells in the treated tumors suppress the inhibitory activity of Tregs (Figure 7b). The combination of immune-stimulatory effects by IFN-α and the reconstitution of a fresh immune system following HSCT could create an environment strongly supporting the activation of an antitumor response. We propose a model showing the integrated mechanisms of inducing a strong antitumor immunity by a combination therapy (Figure 8).

Although the conditioning of HSCT with irradiation and/or immunosuppressive reagents can destroy the immunotolerance deployed by the tumor, the tumors restore a tolerant microenvironment by induction of Tregs and the production of immune-inhibitory cytokines,[18] which may be one of the main reasons for the failure to fully sustain HP-mediated antitumor immunity. An analysis of the cytokine profile unexpectedly showed that the IFN/HSCT-$CD11c^+$ cells produce a large amount of IL-6 as well as other immune-stimulatory cytokines (Figure 6b). It has been reported that IL-6 increases methylation of upstream Foxp3 enhancer and represses the Foxp3 transcription in natural Tregs.[19] Our findings demonstrated that $CD11c^+$ cells isolated from the tumors transduced by *IFN-α* gene significantly suppress the activity of Tregs (Figure 7b), which may inhibit or delay the reconstitution of an immunotolerant microenvironment in the tumor. $CD11c^+$ cells seem to have a capacity to produce IL-6 in response to IFN-α in a dose-dependent manner (Figure 7a). The IL-6 production was increased in the HSCT-$CD11c^+$ cells also (Figures 6b and 7b). The intratumoral IFN-α expression and the immune-stimulatory condition by elevated cytokine levels after synHSCT may synergistically influence $CD11c^+$ cells to produce IL-6. It is also reported that IL-6 promotes carcinogenesis through multiple signal pathways.[20] The role of IL-6 in tumors is probably based on the balance between the positive and negative effect of IL-6 on the tumor growth. Although it is known that DCs secrete proinflammatory cytokines such as IL-6 by toll-like receptor stimulation,[17] further research is needed to clarify the critical factor/pathway for the production of IL-6 from DCs in synHSCT recipients.

As HP leads to a break in tolerance against self-antigens, the expression of IFN-α could theoretically promote T-cell response not only against tumor cells but also against host normal cells, which may cause an autoimmune reaction. However, no overt toxicity was observed for the treated mice, including their blood chemistry. The immunogenic DCs at the IFN-α vector-injected tumor site were able to capture both TAAs and normal self-antigens shared by tumor and normal cells, and promote tumor-specific immunity and a local autoimmune reaction, whereas resting host DCs away from the tumor site present only normal self-antigens and may induce tolerance or exhaustion of host-reactive T cells. Alternatively, we recently found that the percentage of $Foxp3^+$ cells per $CD4^+$ T cells in the spleen was clearly elevated at an early phase after syngeneic HSCT (data not shown), which differed from the low frequency of $Foxp3^+$ T cells in the tumor (Figure 7d). The finding suggests that among $CD4^+$ T cells, Tregs rapidly proliferate during HP in the body, which might protect patients against autoimmunity after autologous HSCT.

There have been several animal studies showing the potential efficacy of gene- and cell-based immunotherapy in syngeneic HSCT mice. The vaccination with syngeneic tumor cells expressing granulocyte-macrophage colony stimulating factor showed a strong antitumor effect in the transplanted mice.[5] An immunization with DCs pulsed with whole tumor cell lysates led to efficient antitumor responses in a mouse breast tumor model.[21] Adoptive transfer of tumor-specific T cells has also shown enhanced antitumor immune responses after HSCT in lymphopenic mice,[2] and recently, Morgan *et al.*[22] reported efficacy of a strategy composed of immunodepletion and adaptive cell transfer for patients with metastatic melanoma. As tumor-reactive T cells are mostly polyclonal, and heterogeneous expressions of various TAAs coexist even in a tumor mass, the *in vivo* stimulation of multiple tumor-reactive lymphocytes might be critical in the clinical application. Moreover, compared with the previous approaches, another major advantage of an *in vivo IFN-α* gene transfer is that it does not involve a manipulation and culture of the immune and tumor cells *ex vivo*, making this strategy more feasible for many patients with solid cancers. We previously reported that an allogeneic MHC gene transfer also could enhance an effective antitumor immunity in HSCT recipients.[6] The major difference between the allogeneic MHC and *IFN-α* gene therapies is in their local effects on tumor sites transduced with the therapeutic genes: *IFN-α* gene transfer significantly induces cell death and growth inhibition (Figure 2b and see Hara *et al.*[12]). In addition, IFN-α seems to have direct effects upon DCs such as the maturation of the cells and production of immune-stimulatory cytokines and enhancement of inhibitory activity against Tregs. Therefore, a local *IFN-α* gene therapy is a promising therapeutic strategy, especially in a case in which cancer conditions need strong local tumor control and systemic antitumor activity.

Some of the experiments in this study showed important points to consider in the clinical feasibility of the combination therapy.

**Figure 4** A large number of IFN-α-producing cells are induced by intratumoral *IFN-α* gene transfer in synHSCT recipient mice. **(a)** Enzyme-linked immunosorbent spot assay of IFN-γ-producing cells in response to stimulation of CT26 cells. At 2 weeks after plasmid-mediated *IFN-α* gene transfer, mouse splenocytes were isolated from treated mice and co-cultured with CT26 cells or control lymphocytes ($n$=3). The experiments were repeated three times. **(b)** Intracellular cytokine staining of IFN-γ-producing cells in response to stimulation of CT26 cells. The splenocytes ($1\times10^6$) from treated mice were incubated with CT26 ($1\times10^5$) and stained by allophycocyanin-anti-mouse IFN-γ. The activated cell fractions were analyzed by staining with fluorescein isothiocyanate-anti-mouse CD4, CD8 or CD49b (labeling NK cell) antibody ($n$=3–4). The experiments were repeated twice. **(c)** *In vitro* cytotoxic assay of splenocytes. Splenocytes were isolated from the treated mice, and their cytotoxicity was evaluated in a standard 4 h $^{51}Cr$ release assay against CT26 cells ($n$=3). The statistical difference between cell lysis in the synHSCT mice with *IFN-α* gene transfer and synHSCT alone mice is presented (left panel). Splenocytes isolated from synHSCT mice with *IFN-α* gene transfer were pre-incubated with the anti-CD4 or anti-CD8 antibodies for 1 h before cytolysis for CT26 cells (right panel). The data are expressed as cell lysis inhibition (%) at E/T ratio=40 (cell lysis with co-incubation of antibody/that with no antibody). The experiments were repeated twice. **(d)** Antitumor effect of *IFN-α* gene transfer after *in vivo* depletion of $CD4^+$ T cells, $CD8^+$ T cells and NK cells. A group of transplanted mice were treated with anti-CD4, anti-CD8 or anti-asialo GM1 antibodies (targeting NK cells) to deplete these cell populations, and the CT26 tumors were injected with pIFN-α vector ($n$=7–9). Tumor volumes at 10 days after *IFN-α* gene transfer are presented.

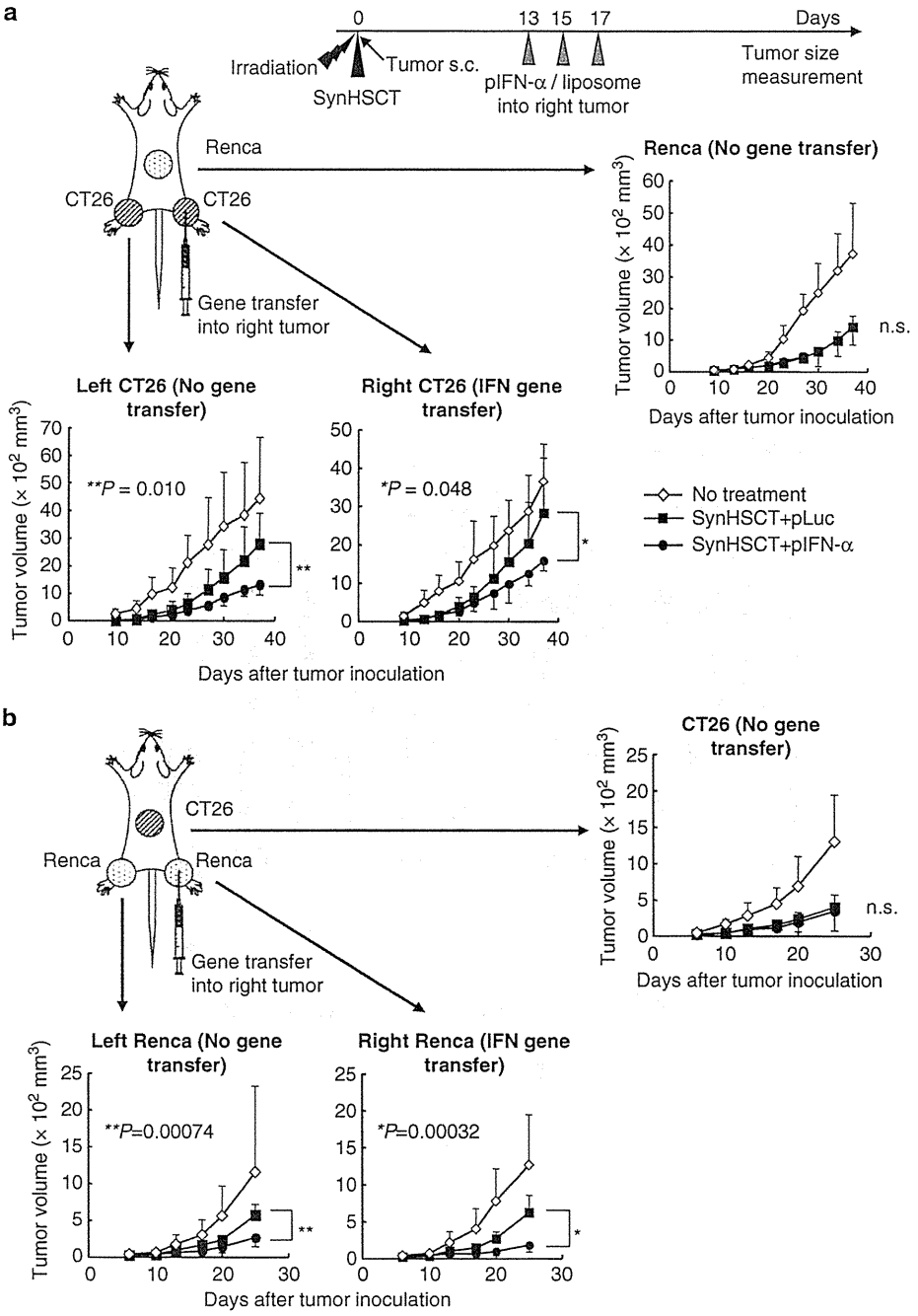


**Figure 5** Suppression of tumors at distant site by *IFN-α* gene transfer during immune reconstitution. The experiments were repeated two times. (**a**) Intratumoral *IFN-α* gene transfer into CT26 tumors. CT26 cells were inoculated on both legs and Renca cells were inoculated on the back in synHSCT mice. The pIFN-α/liposome complex was injected into CT26 subcutaneous tumors on the right legs at days 13, 15 and 17 ($n$=4–8). (**b**) Intratumoral *IFN-α* gene transfer into Renca tumors. Renca cells were inoculated on both legs and CT26 cells on the back in synHSCT mice. The pIFN-α/liposome complex was injected into Renca subcutaneous tumors on the right legs at days 13, 15 and 17 ($n$=4–8). (**c**) Suppression of liver metastasis. CT26-Luc cells were injected beneath the splenic capsule to generate liver metastasis, and CT26 cells were inoculated on the right leg. After the *IFN-α* gene transfer, the size of subcutaneous tumors on the legs was macroscopically measured, and photon count of abdominal tumors was evaluated by the IVIS imaging system. (**d**) *Ex vivo* imaging of the liver. The livers were resected from treated mice at 21 days after the synHSCT, and photon spots and counts of the livers were evaluated by the imaging system. Arrowheads: liver tumors.

First, a liposome-mediated *IFN-α* gene transfer effectively suppressed tumor growth in synHSCT recipients. Although the peak level of IFN-α expression was not very high, the expression continued for more than 10 days after gene transfer (Figure 2d), suggesting that a high concentration of IFN-α in the tumors is not necessary and that the continuous expression is important to induce an effective antitumor

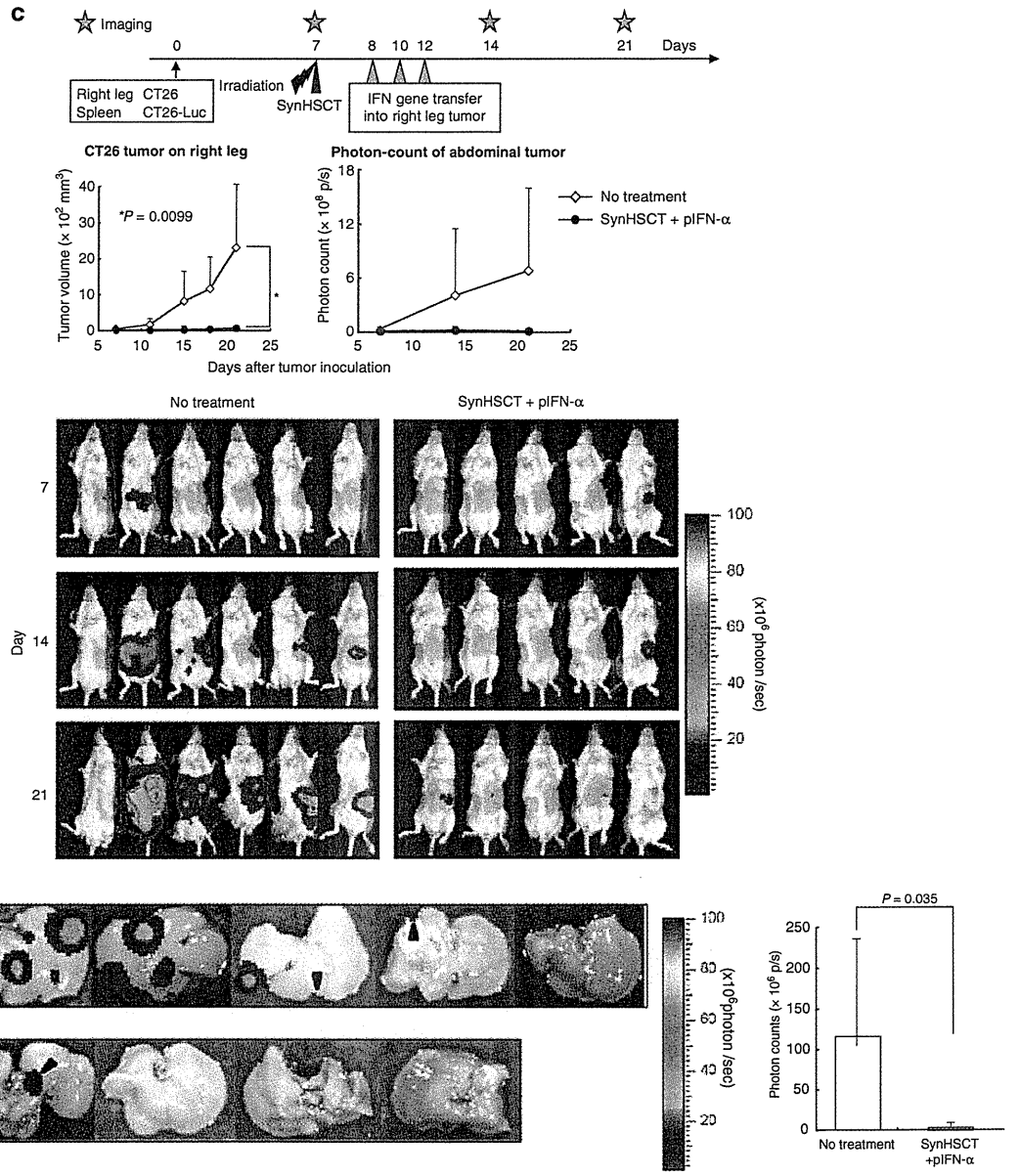


**Figure 5** Continued.

immunity. This facilitates a clinical application, because *in vivo* lipofection of an IFN-α-expressing plasmid is much safer than virus vectors, although the latter has a high gene transduction efficacy.[14] Second, the intratumoral *IFN-α* gene transfer at 6 weeks after synHSCT significantly suppressed tumor growth and prolonged the survival of synHSCT mice (Figures 2e and f). At 6 weeks after synHSCT, neutrophil count returned to a normal level (data not shown), which avoids the risk of bacterial infection that accompanies a needle injection for intratumoral gene transfer. Third, a combination therapy was effective in suppressing not only the vector-injected tumors but also the vector-uninjected distant tumors in the liver metastasis model, which resembles a clinical setting. The results indicated that this treatment strategy might be feasible for many patients with solid cancers. The next step in research may include a further elucidation of the main mechanism of IFN-α in inducing tumor immunity and the synergism between IFN-α and synHSCT, including identification of potential key factors other than IL-6 and DC, development of methods to further sustain and control tumor-specific immunity and to predict and monitor HP followed by an individualization of the combination therapy.

In conclusion, a combination of intratumoral *IFN-α* gene transfer with synHSCT is a promising immunotherapy for solid cancers, because of the activation of tumor-specific immunity, suppression of the immunotolerant environment and excellent safety features. This therapeutic strategy deserves an evaluation in future clinical trial for solid cancers.

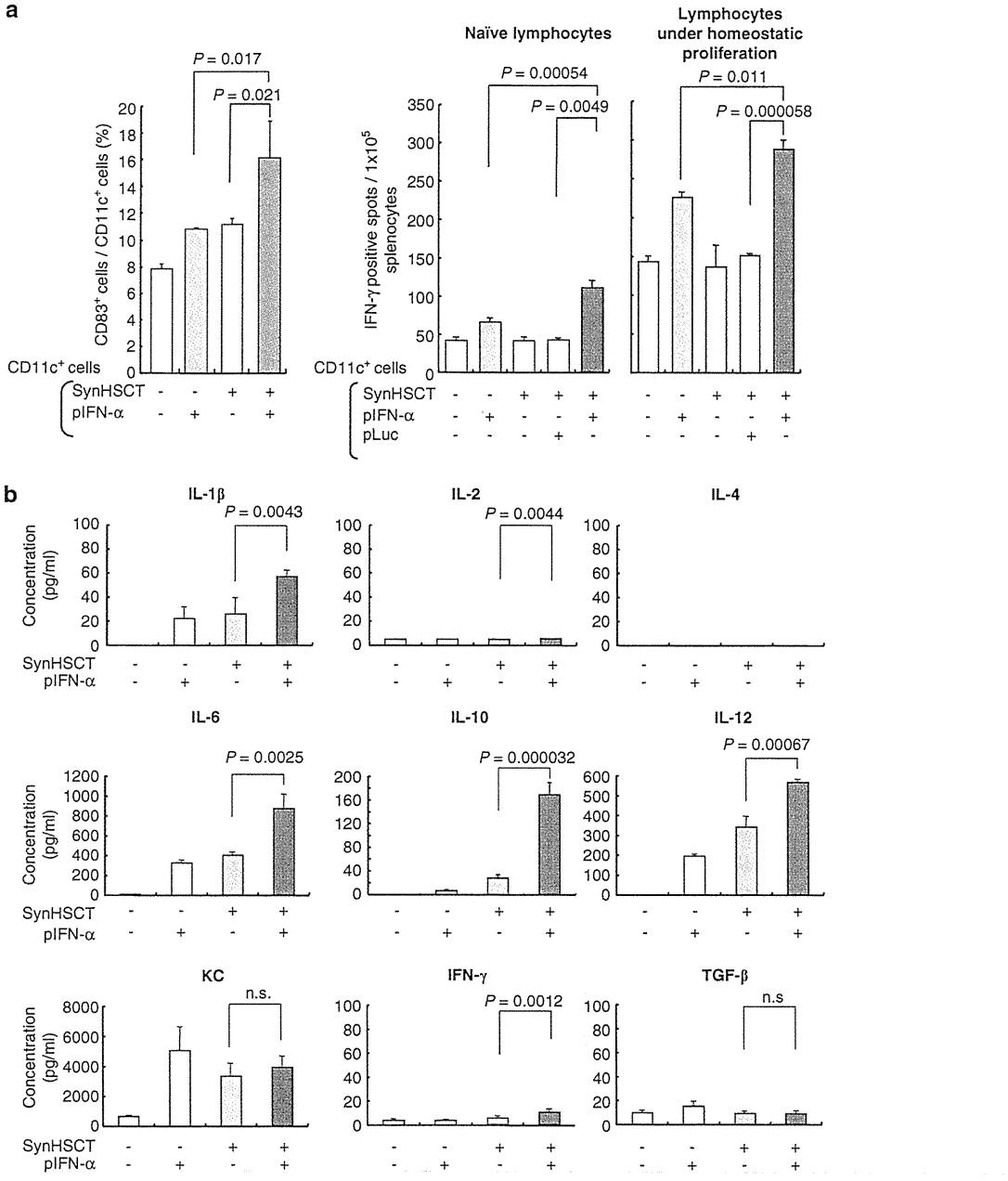


**Figure 6** IFN-α expression promotes the maturation of CD11c$^+$ cells in the tumor. (**a**) Number of IFN-γ-positive cells by enzyme-linked immunosorbent spot assay. Flow cytometry of CD83$^+$ cells (Michel-19; BD Pharmingen) was performed in the CD11c$^+$ cells isolated from tumors ($n$=3). The frequency of CD83$^+$ cells per CD11c$^+$ cells is presented (left panel). CD11c$^+$ cells from treated tumors were co-cultured with lymphocytes isolated from naïve BALB/c mice (middle panel) or synHSCT mice (right panel), and lymphocyte activation was measured by IFN-γ-enzyme-linked immunosorbent spot assay ($n$=3). The experiments were repeated twice. (**b**) Cytokine production of CD11c$^+$ cells. CD11c$^+$ cells were isolated from treated tumors ($n$=3), and were seeded in a 48-well plate ($1\times10^5$ cells per well). After the incubation for 48 h, cytokines in the medium were measured by a cytokine array (Procarta Cytokine Assay Kit; Panomics, Inc., Fremont, CA, USA). IL-10 level was measured by enzyme-linked immunosorbent assay (Quantikine; R&D Systems, Minneapolis, MN, USA). The experiments were repeated three times.

## MATERIALS AND METHODS

### Animals and hematopoietic stem cell transplantation

Seven-to-nine-week-old female BALB/c (H-2$^d$ Ly-1.2) mice were purchased from Charles River Japan, Inc., (Kanagawa, Japan). Animal studies were carried out according to the *Guideline for Animal Experiments of the National Cancer Center Research Institute* and approved by the Institutional Committee for Ethics in Animal Experimentation. Nine-to-ten-week-old BALB/c mice received a lethal (9 Gy) irradiation on the day of transplantation. The irradiated BALB/c mice were injected intravenously with $5\times10^6$ of bone marrow cells and $2\times10^6$ splenic T cells from donor BALB/c mice. Bone marrow cells were isolated from donors by

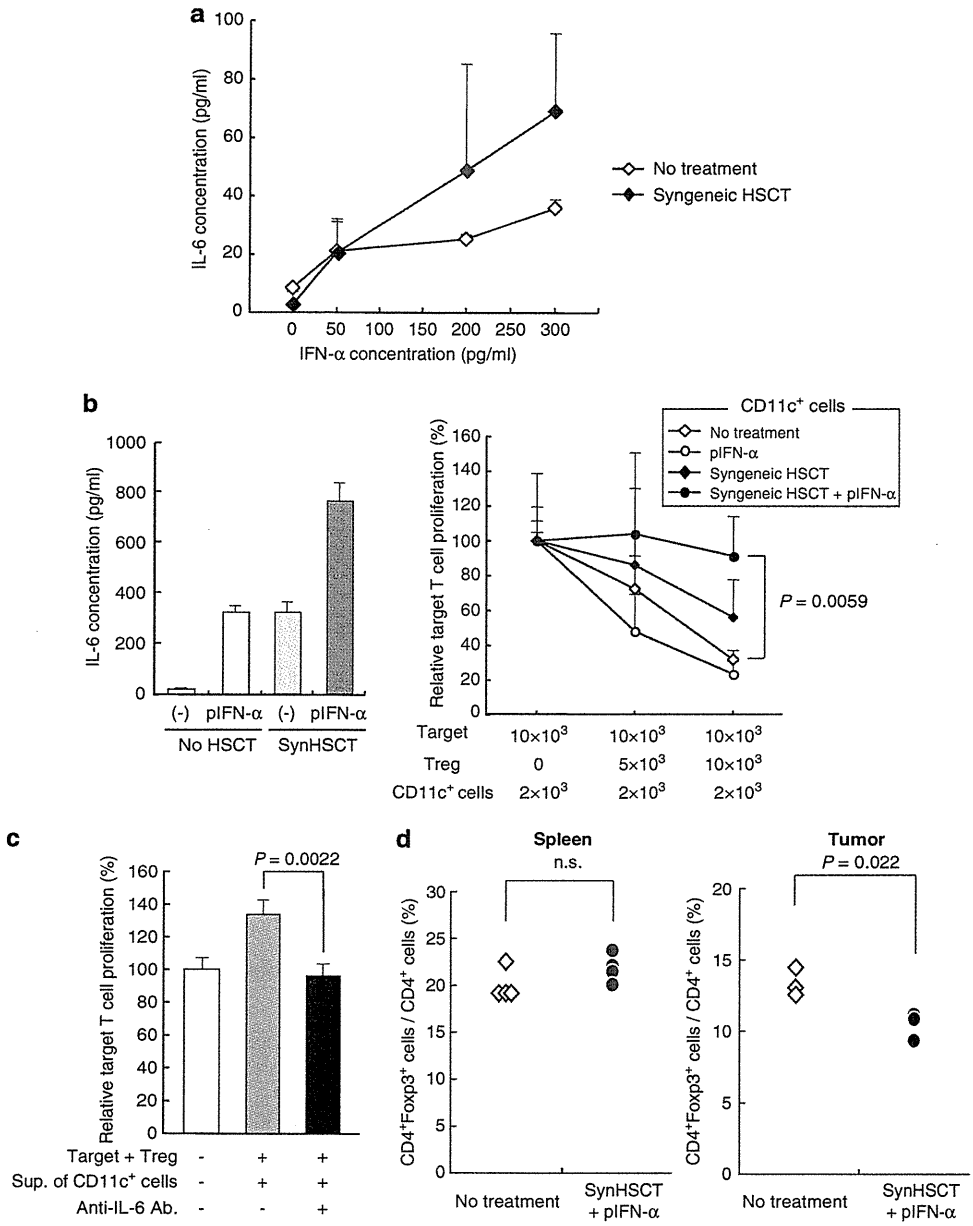


**Figure 7** CD11c$^+$ cells in the tumor inhibit the immunosuppressive activity of Tregs. (**a**) CD11c$^+$ cells produce IL-6 in response to IFN-α. CD11c$^+$ cells isolated from the spleens of non-HSCT and synHSCT tumor-bearing BALB/c mice were seeded in a 96-well plate ($1.5\times10^5$ cells per well) and cultured in the medium containing IFN-α protein at indicated concentration for 2 h. After the change of medium, the cells were incubated for 48 h, and IL-6 in the medium was measured by ELISA (Quantikine; R&D Systems). The experiments were repeated twice. (**b**) The inhibition of activity of Tregs by CD11c$^+$ cells. The CD11c$^+$ cells were isolated from treated tumors and seeded in a 48-well plate ($1\times10^5$ cells per well), and after incubation for 24 h ($n$=4) (left panel), IL-6 production from the CD11c$^+$ cells was measured by ELISA. Target cells (CD4$^+$CD25$^-$ T cell) and Treg (CD4$^+$CD25$^+$ T cell) were isolated from the spleen of naïve BALB/c mice, and were co-cultured with the designated CD11c$^+$ cells in a CD3-coated 96-well plate, and the proliferation of target cells was examined by $^3$H-thymidine uptake assay ($n$=3) (right panel). The experiments were repeated three times. (**c**) IL-6-mediated suppression of Treg activity. Target cells and Tregs were cultured in a CD3-coated 96-well plate with the supernatant of CD11c$^+$cells from treated tumors, and the proliferation of target cells was evaluated by $^3$H-thymidine uptake assay ($n$=3). The addition of anti-IL-6 antibody (R&D systems) was used to neutralize mouse IL-6 in the medium. The experiments were repeated twice. (**d**) The frequency of Tregs in the spleen and treated tumors. The lymphocytes were collected from the spleens ($n$=4, left panel) and treated tumor ($n$=3, right panel), and Foxp3$^+$ and CD4$^+$ cells were analyzed by flow cytometry.

flushing each femur and tibia with RPMI-1640 medium (RPMI) supplemented with 5% heat-inactivated fetal bovine serum (ICN Biomedicals, Inc., Irvine, CA, USA), and splenic cells were prepared by macerating the spleens. After lysis of the erythrocytes, splenic cells were incubated with anti-Thy-1.2 immunomagnetic beads (Miltenyi Biotec GmbH, Bergisch Gladbach, Germany) at 4 °C for 15 min, followed by selection of T cells by AutoMACS (Miltenyi Biotec).

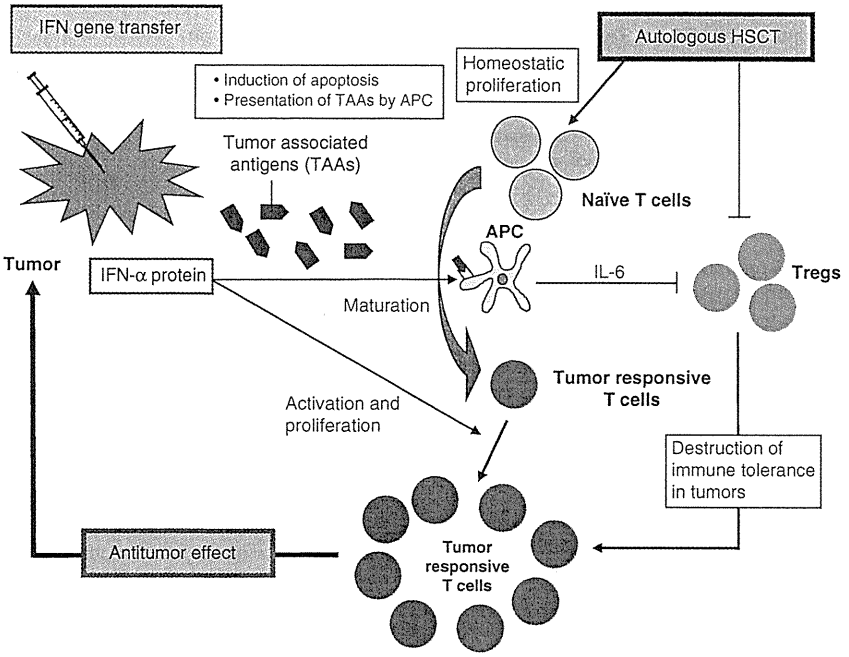


**Figure 8** Model showing integrated mechanisms of inducing strong tumor immunity by a combination therapy. In the 'homeostatic proliferation' condition after synHSCT, T cells effectively recognize the low-affinity self-antigen including TAAs, leading to an induction of antitumor immunity. The conditioning of HSCT with irradiation and/or immunosuppressive reagents can destroy the immunotolerance mechanisms developed by the tumor. Furthermore, IFN-α expression in the tumors exposes TAAs in large quantity to DCs, and IFN-α promotes maturation and enhances the antigen-presenting capacity of DCs. In addition, DCs produced a significant amount of IL-6 in response to IFN-α, which suppress the proliferation and activity of Tregs. The integrated mechanisms are capable of inducing a strong antitumor immunity against solid cancers.

### Tumor cell lines, recombinant adenovirus vectors and plasmid vectors

CT26 and Renca (American Type Culture Collection, Rockville, MD, USA) are weakly immunogenic BALB/c-derived colon and renal cancer cell lines, respectively. Cells were maintained in RPMI containing 10% fetal bovine serum, 2 mM L-glutamine and 0.15% sodium bicarbonate (complete RPMI). A CT26 cell line that stably expresses the firefly luciferase gene was generated by retrovirus vector-mediated transduction and designated as CT26-Luc. The recombinant adenovirus vectors expressing mouse interferon-α (Ad-mIFN) and alkaline phosphatase cDNA (Ad-AP) were prepared as described.[23,24] The recombinant adenoviruses are based on serotype 5 with deletions of the entire E1 and a part of the E3 regions, and have the CAG promoter, which is a hybrid of the cytomegalovirus immediate early enhancer sequence and the chicken β-actin/rabbit β-globin promoter. A cesium chloride-purified virus was desalted using a sterile Bio-Gel P-6 DG chromatography column (Econopac DG 10; Bio-Rad, Hercules, CA, USA) and diluted for storage in a 13% glycerol/phosphate-buffered saline solution. All viral preparations were confirmed by PCR assay to be free of $E1^+$ adenovirus. A plasmid DNA (pIFN-α) expressing the *IFN-α* gene under the control of the CAG promoter was also used for intratumoral gene transfer. The plasmids that express an alkaline phosphatase (pAP) or luciferase gene (pLuc) were used as a negative control.

### *In vitro* cell proliferation assay

Cultured cells were seeded at $2\times10^3$ per well in 96-well plates and plasmid DNA-liposome (Lipofectamine2000; Invitrogen, Carlsbad, CA, USA) complex was added according to the manufacturer's protocol. The cell numbers were assessed by a colorimetric cell viability assay using a water-soluble tetrazolium salt (Tetracolor One; Seikagaku Corp., Tokyo, Japan) at 5 days after the transfection. Absorbance was determined by spectrophotometry using a wavelength of 450 nm with 595 nm as a reference. The assays (carried out in four wells) were repeated three times.

### *In vivo* tumor inoculation and *IFN-α* gene transfer

CT26 cells ($1\times10^6$) or Renca cells ($5\times10^6$) were injected subcutaneously into the leg of BALB/c mice. When the subcutaneous tumor was established (~0.6 cm in diameter), it was injected once with 50 μl of Ad-mIFN or control vector (Ad-AP). Plasmid DNA–liposome complex was prepared by the addition of 30 μg plasmid DNA into a total of 75 μl phosphate-buffered saline per mouse, followed by the addition of 75 μl of 0.15 mmol $l^{-1}$ DMRIE-DOPE ((+/−)-*N*-(2-hydroxyethyl)-*N*, *N*-dimethyl –2,3-bis(tetradecyloxy)-1-propanaminium bromide/dioleoylphosphatidylethanolamine), which was provided from Vical, Inc., (San Diego, CA, USA). The mixture solution was incubated at room temperature for 15 min, and then injected directly into the tumor three times every other day. The shortest ($r$) and longest ($l$) tumor diameters were measured at indicated days and the tumor volume was determined as $r^2l/2$. Data are presented as mean ± s.d. The experiments were repeated two times.

### Enzyme-linked immunosorbent spot assays

IFN-γ ELISpot kit (BD Bioscience, San Jose, CA, USA) was used according to the manufacturer's instructions. Briefly, splenocytes ($1\times10^5$) and mitomycin C-treated tumor cells ($1\times10^4$) were co-cultured in 96-well plates pre-coated with mouse IFN-γ (BD Bioscience) for 20 h at 37 °C in complete RPMI medium in triplicate. After washing the wells, biotinylated anti-mouse IFN-γ antibody (2 μg $ml^{-1}$) was added and incubated for 2 h at room temperature. Then, a streptavidin-horseradish peroxidase solution was added and incubated for 1 h at room temperature. After the addition of an aminoethyl carbozole substrate solution, spots were counted under a stereomicroscope.

### Flow cytometry of cell surface marker and intracellular cytokine staining

Allo-phycocyanin-conjugated monoclonal antibody (mAb) to identify mouse IFN-γ and fluorescein isothiocyanate-conjugated mAb to detect CD4, CD8 and CD49b were purchased from BD Pharmingen (San Jose, CA, USA). Splenocytes ($1\times10^6$) were incubated with medium alone (control) or CT26 ($1\times10^5$) cells

for 2 days; brefeldin-A (10 μg ml$^{-1}$) was then added for 2 h of incubation. After washing, cells were incubated with the CD4, CD8 or CD49b mAbs in a total volume of 100 μl phosphate-buffered saline with 5% fetal bovine serum for 30 min at 4 °C, and then fixed and permeabilized with a permeabilization buffer (BD Biosciences). Cells were finally stained with antibody to IFN-γ for 15 min at room temperature, washed again and analyzed by FACSCalibur (BD Biosciences). Irrelevant immunoglobulin G mAbs were used as a negative control. Ten thousand live events were acquired for analysis.

### Cytotoxic assays

An *in vitro* cytotoxic assay was performed as previously described.[12] Briefly, splenocytes were cultured for 4 days with mitomycin C-treated CT26 stimulators, and then the responder cells were collected and used as effector cells. CT26 target cells were labeled with $^{51}$Cr (Perkin-Elmer Japan Co., Kanagawa, Japan). For a 4 h chromium release assay, $4\times10^5$, $1\times10^5$ and $5\times10^4$ effector cells were mixed with $1\times10^4$ target cells in a 96-well round-bottom plate (Corning Incorporated, New York, NY, USA). To evaluate the relative contributions of CD4$^+$ and CD8$^+$ T cells for the tumor cell lysis, effector cells were incubated with mAbs against mouse CD4 (L3L4; BD Pharmingen) or CD8 (Ly-2; BD Pharmingen) for 1 h at 37 °C before mixing with target cells. Supernatants were harvested and counted in a gamma counter (Packard Bioscience Company, Meriden, CT, USA). The percentage of cytotoxicity was calculated as ((experimental c.p.m.–spontaneous c.p.m.)/(maximum c.p.m.–spontaneous c.p.m.))×100. Each assay was carried out in triplicate.

### Immunohistochemistry

Immunostaining was performed using streptavidin-biotin-peroxidase complex techniques (Nichirei, Tokyo, Japan). Consecutive cryostat tissue sections (6 μm) were mounted on glass slides and fixed in 99.5% ethanol for 20 min. After blocking with normal rat serum, the sections were stained with rat anti-mouse CD4 and CD8 antibodies (BD Pharmingen). Parallel negative controls with antibodies of the same isotype were examined in all cases. The sections were counter-stained with methyl green.

### *In vivo* depletion of T and NK cells

To deplete the subsets of immune effector cells before and during the treatment with *IFN-α* gene transfer, the synHSCT mice received intraperitoneal injections of 0.3 mg. Monoclonal antibody from the anti-CD4$^+$ hybridoma (clone GK1.5, rat IgG2b) or 1.5 mg mAb from the anti-CD8$^+$ hybridoma (clone Lyt–2.1, mouse IgG2b; see Nakayama and Uenaka[25]) or 0.5 mg of anti-asialo GM1 antibody (targeting NK cells: Wako Pure Chemical Industries, Ltd, Tokyo, Japan). Administration of antibodies started at 2 days after the inoculation of CT26 cells, and the injection was repeated every 5–6 days, throughout the entire experimental period. Flow cytometry showed that ~80% of CD4$^+$, ~60% of CD8$^+$ T cells and ~80% of NK cells were depleted in the Ab-treated mice.

### *In vivo* imaging of the tumors in a liver-metastasis model

CT26-Luc cells were injected beneath the splenic capsule to generate liver metastasis. The BALB/c mice with CT26-Luc tumors were administered with D-luciferin (150 mg kg$^{-1}$) (Wako Pure Chemical Industries) by intraperitoneal injection. At 10 min later, photons from animal whole bodies were counted using an *in vivo* imaging system.

### Isolation of CD11c+ cells and T-cell proliferation assay

Dendritic cells were isolated using mouse CD11c MicroBeads and AutoMACS magnetic sorter (Miltenyi Biotec) from tumors of non-HSCT mice treated by intratumoral *IFN-α* gene transfer, tumors of synHSCT mice injected with control plasmid and tumors of synHSCT mice treated by intratumoral *IFN-α* gene transfer, and designated as IFN-CD11c$^+$, HSCT-CD11c$^+$ and IFN/HSCT-CD11c$^+$, respectively. The flow cytometry showed that ~90% of isolated cells express CD11c, and that ~80% of the isolated CD11c$^+$ cells are negative for CD14 (macrophage marker), suggesting that a major population of isolated CD11c$^+$ cells is DCs. CD4$^+$CD25$^+$ or CD4$^+$CD25$^-$ T cells were isolated from the spleen of naïve BALB/c mice using mouse CD4 pre-enrichment kit, mouse CD25 selection kit and RoboSep magnetic sorter (StemCell Technologies, Vancouver, BC, Canada). These populations were stained with anti-Foxp3 antibody, and flow cytometry revealed that about 80% of CD4$^+$CD25$^+$cells expressed Foxp3. CD4$^+$CD25$^-$ T cells were incubated in a 96-well plate ($1\times10^4$ per well) with $2\times10^3$ of CD11c$^+$ cells, 0.5 μg ml$^{-1}$ of anti-CD3 antibody and the indicated number of CD4$^+$CD25$^+$ T cells for 48 h. T-cell proliferation was determined as $^3$H-thymidine incorporation during the last 12 h of culture.

### Statistical analysis

Comparative analyses of the data were performed by the Student's *t*-test, using SPSS statistical software (SPSS Japan Inc., Tokyo, Japan). $P<0.05$ was considered as a significant difference.

## CONFLICT OF INTEREST

The authors declare no conflict of interest.

## ACKNOWLEDGEMENTS

This work was supported in part by a grant-in-aid for the 3rd Term Comprehensive 10-year Strategy for Cancer Control from the Ministry of Health, Labour and Welfare of Japan, by grants-in-aid for Cancer Research from the Ministry of Health, Labour and Welfare of Japan and by the program for promotion of Foundation Studies in Health Science of the National Institute of Biomedical Innovation (NIBIO) and by Kobayashi Foundation for Cancer Research. H Hara and T Udagawa are awardees of a Research Resident Fellowship from the Foundation for Promotion of Cancer Research. We thank Vical Incorporated for providing the DMRIE/DOPE liposome.

1 Rabinovich GA, Gabrilovich D, Sotomayor EM. Immunosuppressive strategies that are mediated by tumor cells. *Annu Rev Immunol* 2007; **25**: 267–296.
2 Wrzesinski C, Restifo NP. Less is more: lymphodepletion followed by hematopoietic stem cell transplant augments adoptive T-cell-based anti-tumor immunotherapy. *Curr Opin Immunol* 2005; **17**: 195–201.
3 Hu HM, Poehlein CH, Urba WJ, Fox BA. Development of antitumor immune responses in reconstituted lymphopenic hosts. *Cancer Res* 2002; **62**: 3914–9391.
4 Dummer W, Niethammer AG, Bacccala R, Lawson BR, Wagner N, Reisfeld RA *et al.* T cell homeostatic proliferation elicits effective antitumor autoimmunity. *J Clin Invest* 2002; **110**: 185–192.
5 Borrello I, Sotomayor EM, Rattis FM, Cooke SK, Gu L, Levitsky HI. Sustaining the graft-versus-tumor effect through posttransplant immunization with granulocyte-macrophage colony-stimulating factor (GM-CSF)-producing tumor vaccines. *Blood* 2000; **95**: 3011–3019.
6 Kobayashi A, Hara H, Ohashi M, Nishimoto T, Yoshida K, Ohkohchi N *et al.* Allogeneic MHC gene transfer enhances an effective antitumor immunity in the early period of autologous hematopoietic stem cell transplantation. *Clin Cancer Res* 2007; **13**: 7469–7479.
7 Pfeffer LM, Dinarello CA, Herberman RB, Williams BR, Borden EC, Bordens R *et al.* Biological properties of recombinant α-Interferons: 40$^{th}$ anniversary of the discovery of interferons. *Cancer Res* 1998; **58**: 2489–2499.
8 Belardelli F, Ferrantini M, Proietti E, Kirkwood JM. Interferon-alpha in tumor immunity and immunotherapy. *Cytokine Growth Factor Rev* 2002; **13**: 119–134.
9 Santini SM, Lapenta C, Santodonato L, D'Agostino G, Belardelli F, Ferrantini M. IFN-alpha in the generation of dendritic cells for cancer immunotherapy. *Handb Exp Pharmacol* 2009; **188**: 295–317.
10 Ferrantini M, Capone I, Belardelli F. Dendritic cells and cytokines in immune rejection of cancer. *Cytokine Growth Factor Rev* 2008; **19**: 93–107.
11 Hara H, Kobayashi A, Yoshida K, Ohashi M, Ohnami S, Uchida E *et al.* Local interferon-α gene therapy elicits systemic immunity in a syngeneic pancreatic cancer model in hamster. *Cancer Sci* 2007; **98**: 455–463.
12 Hara H, Kobayashi A, Narumi K, Kondoh A, Yoshida K, Nishimoto T *et al.* Intratumoral interferon-α gene transfer enhances tumor immunity after allogeneic hematopoietic stem cell transplantation. *Cancer Immunol Immunother* 2009; **58**: 1007–1021.
13 Narumi K, Kondoh A, Udagawa T, Hara H, Goto N, Ikarashi Y *et al.* Administration route-dependent induction of antitumor immunity by interferon-alpha gene transfer. *Cancer Sci* 2010; **101**: 1686–1694.
14 Rodriguez EG. Nonviral DNA vectors for immunization and therapy: design and methods for their obtention. *J Mol Med* 2004; **82**: 500–509.
15 Ohtani H. Focus on TILs: prognostic significance of tumor infiltrating lymphocytes in human colorectal cancer. *Cancer Immunity* 2007; **7**: 4–13.
16 Garcia CA, Wang H, Benakanakere MR, Barrett E, Kinane DF, Martin M. c-Jun controls the ability of IL-12 to induce IL-10 production from human memory CD4$^+$ T cells. *J Immunol* 2009; **183**: 4475–4482.
17 Pasare C, Medzhitov R. Toll pathway-dependent blockade of CD4$^+$CD25$^+$ T-cell-mediated suppression by dendritic cells. *Science* 2003; **299**: 1033–1036.

18 Curiel TJ, Coukos G, Zou L, Alvarez X, Cheng P, Mottram P *et al.* Specific recruitment of regulatory T cells in ovarian carcinoma fosters immune privilege and predicts reduced survival. *Nat Med* 2004; **10**: 942–949.
19 Lai G, Zhang N, van der Touw W, Ding Y, Ju W, Bottinger EP *et al.* Epigenetic regulation of Foxp3 expression in regulatory T cells by DNA methylation. *J Immunol* 2009; **182**: 259–273.
20 Grivennikov S, Karin E, Terzic J, Mucida D, Yu GY, Vallabhapurapu S *et al.* IL-6 and Stat3 are required for survival of intestinal epithelial cells and development of colitis-associated cancer. *Cancer Cell* 2009; **15**: 103–113.
21 Asavaroengchai W, Kotera Y, Mule JJ. Tumor lysate-pulsed dendritic cells can elicit an effective antitumor immune response during early lymphoid recovery. *Proc Natl Acad Sci USA* 2002; **99**: 931–936.
22 Morgan RA, Dudley ME, Wunderlich JR, Hughes MS, Yang JC, Sherry RM *et al.* Cancer regression in patients after transfer of genetically engineered lymphocytes. *Science* 2006; **314**: 126–129.
23 Aoki K, Barker C, Danthinne X, Imperiale MJ, Nabel GJ. Efficient generation of recombinant adenoviral vectors by Cre-lox recombination *in vitro*. *Mol Med* 1999; **5**: 224–231.
24 Ohashi M, Yoshida K, Kushida M, Miura Y, Ohnami S, Ikarashi Y *et al.* Adenovirus-mediated interferon α gene transfer induces regional direct cytotoxicity and possible systemic immunity against pancreatic cancer. *Br J Cancer* 2005; **93**: 441–449.
25 Nakayama E, Uenaka A. Effect of *in vivo* administration of Lyt antibodies. *J Exp Med* 1985; **161**: 345–355.

THE JOURNAL OF BIOLOGICAL CHEMISTRY VOL. 287, NO. 2, pp. 1397–1405, January 6, 2012


# Competitive Interactions of Cancer Cells and Normal Cells via Secretory MicroRNAs*[S]

Received for publication, August 4, 2011, and in revised form, November 23, 2011 Published, JBC Papers in Press, November 28, 2011, DOI 10.1074/jbc.M111.288662

**Nobuyoshi Kosaka**[‡1], **Haruhisa Iguchi**[‡§1], **Yusuke Yoshioka**[‡2], **Keitaro Hagiwara**[‡¶], **Fumitaka Takeshita**[‡], **and Takahiro Ochiya**[‡3]

*From the* [‡]*Division of Molecular and Cellular Medicine, National Cancer Center Research Institute, 5-1-1, Tsukiji, Chuo-ku, Tokyo 104-0045, Japan,* [§]*Pharmacology Research Laboratories, Dainippon Sumitomo Pharma Co., Ltd., 1-98, Kasugadenaka 3-chome, Konohana-ku, Osaka 554-0022, Japan, and the* [¶]*Department of Biological Information, Graduate School of Bioscience and Biotechnology, Tokyo Institute of Technology, Yokohama, Kanagawa 226-8501, Japan*

**Background:** Homeostatic cell competitive system between cancerous cells and non-cancerous cells is considered as the reason for tumor initiation.
**Results:** Exosomal tumor-suppressive microRNAs secreted by non-cancerous cells inhibit the proliferation of cancerous cells.
**Conclusion:** Exosomal tumor-suppressive microRNAs act as an inhibitory signal for cancer cells in a cell-competitive process.
**Significance:** This provides a novel insight into a tumor initiation mechanism.

**Normal epithelial cells regulate the secretion of autocrine and paracrine factors that prevent aberrant growth of neighboring cells, leading to healthy development and normal metabolism. One reason for tumor initiation is considered to be a failure of this homeostatic cell competitive system. Here we identify tumor-suppressive microRNAs (miRNAs) secreted by normal cells as anti-proliferative signal entities. Culture supernatant of normal epithelial prostate PNT-2 cells attenuated proliferation of PC-3M-luc cells, prostate cancer cells. Global analysis of miRNA expression signature revealed that a variety of tumor-suppressive miRNAs are released from PNT-2 cells. Of these miRNAs, secretory miR-143 could induce growth inhibition exclusively in cancer cells *in vitro* and *in vivo*. These results suggest that secretory tumor-suppressive miRNAs can act as a death signal in a cell competitive process. This study provides a novel insight into a tumor initiation mechanism.**

Competitive interactions among cells are the basis of many homeostatic processes in biology. In *Drosophila*, normal epithelial cells compete with transformed ones for individual survival, which is a process called cell competition (1, 2). If a given group of cells was exposed to some stress, it would be separated into subpopulations of cells with different levels of damage. In noncompetitive conditions, cells with severe damage die in a short time, whereas moderately damaged cells survive to the next generation, indicative of the transduction of a negative phenotype. On the other hand, in competitive conditions even slightly damaged cells are eliminated from the cell group because healthy cells, the "winners," convey death signals to damaged cells, the "losers," and the losers reciprocally confer growth signals to the winners. This feed-forward regulation enables the cell population to eradicate abnormal cells and maintain the same number of normal cells in a limited niche.

Oncogenesis is characterized by genetic and metabolic changes reprogramming living cells to undergo uncontrolled proliferation (3). This suggests that the abnormal cells that are originally destined for elimination can survive and expand against the cell competitive regulation, leading to the formation of a tumor mass. Consistently with this concept, Bondar and Medzhitov (4) showed that the cell competition process involves p53, a tumor-suppressive gene, between the hematopoietic stem cells and progenitor cells, suggesting that gene modifications of p53 could disturb the homeostatic mechanism and give rise to tumor initiation. It is conceivable that p53 target genes could be associated with intercellular communication between winners and losers; however, this literature has not answered the question of whether this regulatory system is mediated by contact-dependent or contact-independent manner. More than 10 years ago a pioneer study suggested that non-cancerous cells co-cultured with cancer cells inhibit the growth of cancer cells *in vitro* (5). This result indicated that humoral factors could be involved in cell competition as intercellular communicators (6).

As recently as a few years ago it was believed that RNAs could not behave as extracellular signal molecules because of their vulnerability to the attack of ribonucleases largely existing in body fluid. Evidence is presently increasing to show that miRNAs[4] contained in exosomes are released from mammalian

* This work was supported in part by a grant-in-aid for the Third-Term Comprehensive 10-Year Strategy for Cancer Control, a grant-in-aid for Scientific Research on Priority Areas Cancer from the Ministry of Education, Culture, Sports, Science, and Technology, the Program for Promotion of Fundamental Studies in Health Sciences of the National Institute of Biomedical Innovation, and the Japan Society for the Promotion of Science through the "Funding Program for World-Leading Innovative R&D on Science and Technology (FIRST Program)" initiated by the Council for Science and Technology Policy.
[S] This article contains supplemental Figs. 1–3.
[1] Both authors contributed equally to this work.
[2] A Research Fellow of the Japan Society for the Promotion of Science.
[3] To whom correspondence should be addressed: Division of Molecular and Cellular Medicine, National Cancer Center Research Institute, 1-1, Tsukiji, 5-chome, Chuo-ku, Tokyo 104-0045, Japan. Tel.: 81-3-3542-2511 (ext. 4800); Fax: 81-3-3541-2685; E-mail: tochiya@ncc.go.jp.

[4] The abbreviations used are: miRNA, microRNA; CM, conditioned medium; luc, luciferase; MTT, 3-(4,5-dimethylthiazol-2-yl)-2,5-diphenyltetrazolium bromide; QRT-PCR, quantitative real time PCR.

cells and act as a signal transducer (7). It is important that many different tumor-suppressive miRNAs, such as miR-16 and miR-143, are down-regulated in cancer cells, resulting in tumorigenesis, tumor progression, and metastasis (8–11). Taken together, these findings suggest that secretory miRNAs may have favorable aspects for anti-proliferative signals mediating cell competition.

In this report we show that miR-143 expression in normal prostate cells, PNT-2 cells, is higher than that in prostate cancer cells, PC-3M-luc cells, and that miR-143 released from non-cancerous cells transfers growth-inhibitory signals to cancerous cells *in vitro* and *in vivo*. These results suggest that secretory tumor-suppressive miRNAs might be a death signal from winners to losers in the context of cell competition. Secretory miRNAs can be conducive to the maintenance of normal growth and development.

## EXPERIMENTAL PROCEDURES

*Reagents*—Mouse monoclonal anti-KRAS (F234) (sc-30) was purchased from Santa Cruz. Rabbit polyclonal anti-ERK5 (#3372) was purchased from Cell Signaling. Mouse monoclonal anti-actin, clone C4 (MAB1501), was obtained from Millipore. Mouse monoclonal ant-human-CD63 antibody (556019) was purchased from BD Pharmingen. Peroxidase-labeled anti-mouse and anti-rabbit antibodies were included in the Amersham Biosciences ECL PLUS Western blotting Reagents Pack (RPN2124) (GE Healthcare). Synthetic *Caenorhabditis elegans* miRNA cel-miR-39 was synthesized by Qiagen (Valencia, CA). Synthetic hsa-miR-143 (pre-miR-143), the negative control 1 (NC1), has-miR-143 inhibitor molecule (anti-miR-143), and the negative control inhibitor molecule (anti-NC) were purchased from Ambion (Austin, TX). GW4869 was purchased from Calbiochem. Geneticin was purchased from Invitrogen.

*Cell Culture*—PNT-2 cells, immortalized normal adult prostatic epithelial cell line, were purchased from the DS Pharma Biomedical Co., Ltd. (Osaka, Japan). HEK293 cells, a human embryonic kidney cell line (CRL-1573), were obtained from American Type Culture Collection (Manassas, VA). HEK293 cells were cultured in Dulbecco's modified Eagle's medium containing 10% heat-inactivated fetal bovine serum (FBS) and an antibiotic-antimycotic (Invitrogen) at 37 °C in 5% $CO_2$. PNT-2 and the prostate cancer cell line, PC-3M-luc cells, continuously expressing firefly luciferase (Xenogen, Alameda, CA), were cultured in RPMI containing 10% heat-inactivated FBS and an antibiotic-antimycotic at 37 °C in 5% $CO_2$.

*Preparation of Conditioned Medium and Exosomes*—Before the collection of culture medium, cells were washed 3 times with Advanced RPMI containing an antibiotic-antimycotic and 2 mM L-glutamine (medium A), and the medium was switched to fresh medium A. After incubation for 3 days, medium A was collected and centrifuged at 2000 × *g* for 10 min at room temperature. To thoroughly remove cellular debris, the supernatant was centrifuged again at 12,000 × *g* for 30 min at room temperature or filtered through a 0.22-μm filter (Millipore). The conditioned medium (CM) was then used for miRNA extraction and functional assays as well as exosome isolation.

For exosome preparation the CM was ultracentrifuged at 110,000 × *g* for 70 min at 4 °C. The pellets were washed with 11 ml of PBS, and after ultracentrifugation they were resuspended in PBS. The exosome fraction was measured for its protein content using the Micro BCA Protein Assay kit (Thermo Scientific, Wilmington, DE).

*Isolation of MicroRNAs*—Isolation of extracellular and cellular miRNAs was performed using the miRNeasy Mini Kit (Qiagen). Two hundred microliters of conditioned medium or cell lysate was diluted with 1 ml of Qiazol Solution. After 5 min of incubation, 10 μl of 0.1 nM cel-miR-39 was added to each aliquot followed by vortexing for 30 s. Subsequent extraction and filter cartridge work were carried out according to the manufacturer's protocol.

*Quantitative Real Time PCR (QRT-PCR)*—The method for QRT-PCR has been previously described (7). PCR was carried out in 96-well plates using the 7300 Real Time PCR System (Applied Biosystems). All reactions were done in triplicate. All TaqMan MicroRNA Assays were purchased from Applied Biosystems. Cel-miR-39 and RNU6 were used as an invariant control for the CM and cells, respectively.

*Immunoblot Analysis*—SDS-PAGE gels, SuperSep Ace 5–20% (194–15021) (Wako), were calibrated with Precision Plus Protein Standards (161–0375) (Bio-Rad), and anti-KRAS (1:100), anti-ERK5 (1:1000), anti-CD63 (1:200), and anti-actin (1:1000) were used as primary antibodies. The dilution ratio of each antibody is indicated in parentheses. Two secondary antibodies (peroxidase-labeled anti-mouse and anti-rabbit antibodies) were used at a dilution of 1:10,000. Bound antibodies were visualized by chemiluminescence using the ECL PLUS Western blotting detection System (RPN2132) (GE Healthcare), and luminescent images were analyzed by a LuminoImager (LAS-3000; Fuji Film, Inc.). Only gels for CD63 (BD Biosciences) detection were run under non-reducing conditions.

*Plasmids*—The primary-miR-143 expression vector was purchased from TaKaRa BIO. For luciferase-based reporter gene assays, pLucNeo was constructed by inserting a firefly luciferase gene derived from the pGL3-control (Promega) into the pEYFP-1 vector (Clontech) at BglII and AflII sites. The sensor vector for miR-143 was constructed by introducing tandem binding sites with perfect complementarity to miR-143 separated by a four-nucleotide spacer into the NotI site of psiCHECK2 (Promega). The sequences of the binding site are as follows: 5′-AAACCTAGAGCGGCCGCGAGCTACAGTGCT***TCATCTC***AAAGAATTCTTGAGCTACAGTGCT***TCATCTC***AGCGGCCGCTGGCCGCAA-3′ (sense) and 5′-TTGCGGCCAGCGGCCGCTGAGATGAAGCACTGTAGCTCAAGAATTCTTTGAGATGAAGCACTGTAGCTCGCGGCCGCTCTAGGTTT-3′ (antisense). The "seed" sequence of miR-143 is indicated by bold italics. In a mutated miR-143 sensor vector, the seed sequence, TCATCTC, was displaced with GACGAGA. All the plasmids were verified by DNA sequencing.

*Transient Transfection Assays*—Transfections of 10 nM miR-143 mimic and 3 nM anti-miR-143 were accomplished with the DharmaFECT Transfection Reagent (Thermo Scientific) according to the manufacturer's protocol. The total amounts of miRNAs for each transfection were equally adjusted by the addition of NC1 and anti-NC, respectively.

*Establishment of Stable Cell Lines*—Stable HEK293 cell lines that express miR-143 were generated by selection with 300 μg/ml Geneticin. HEK293 cells were transfected with 0.5 μg of the pri-miR-143 expression vector at 90% confluency in 24-well dishes using a Lipofectamine LTX reagent in accordance with the manufacturer's instructions. Twelve hours after the transfection, the cells were re-plated in a 10-cm dish followed by a 3-week selection with the antibiotic. Ten surviving single colonies were picked up from each transfectant and then cultured for another 2 weeks. The cells expressing the largest amount of miR-143 among transfectants were used as miR-143 stably expressing cells.

*Luciferase Reporter Assay*—HEK293 cells were cultured at a density of $1 \times 10^4$ cells/well in 96-well tissue culture plates overnight, and miRNA transfections or the addition of CM was performed. The cells were harvested, and renilla luciferase activity was measured and normalized by firefly luciferase activity (10). All assays were performed in triplicate and repeated at least three times, and the most representative results are shown.

*Cell Growth Assay*—PC-3M-luc cells were seeded at a density of $2 \times 10^3$ cells/well in a 96-well plate. The following day the cells were transfected with mature miRNAs or incubated with a CM. Twenty-four hours later the culture medium of the transfected cells was switched to medium A, whereas the conditioned medium was not changed. After a 3-day culture, cells were harvested for the measurement of firefly luciferase activity. To know the cellular proliferation by the tetrazolium-based colorimetric MTT assay, 20 μl CM of TetraColor ONE (SEIKAGAKU Corp., Tokyo, Japan) was added to each well after 72 h of culture. After 2–4 h of incubation at 37 °C, the optical density was measured at a wavelength of 450 nm using a microplate reader.

*PKH67-labeled Exosome Transfer*—Purified exosomes derived from PNT-2 CM were labeled with a PKH67 green fluorescent labeling kit (Sigma). Exosomes were incubated with 2 μM PKH67 for 5 min, washed 4 times using a 100-kDa filter (Microcon YM-100, Millipore) to remove excess dye, and incubated with PC-3M-luc cells at 37 °C.

*Co-culture Experiment*—In co-culture experiments, $2 \times 10^5$ cells/well of PNT-2 cells were plated in 6-well plates. To stain the PNT-2 cells with BODIPY-TR-ceramide (Invitrogen), 5 μM BODIPY-TR-ceramide in a non-serum culture medium was added and incubated with the cells at 37 °C. After 30 min the cells were rinsed several times with a non-serum culture medium and incubated in a fresh medium at 37 °C for an additional 30 min. After the staining of PNT-2 cells by BODIPY-TR-ceramide, labeling of PC-3M-luc cells with PKH67 was performed in accordance with the manufacturer's instructions. After that, labeled PC-3M-luc cells were added and co-cultured with PNT-2 cells for 12 h at 37 °C.

*Microarray Analysis*—To detect the miRNAs in exosomes and cells derived from PNT-2 and PC-3M-luc cells, 100 ng of total RNA was labeled and hybridized using a human microRNA microarray kit (Agilent Technologies) according to the manufacturer's protocol (Protocol for Use with Agilent MicroRNA Microarrays Version 1.5). Hybridization signals were detected using a DNA microarray scanner (Agilent Technologies), and the scanned images were analyzed using Agilent Feature Extraction software.

*Evaluation of Tumor-suppressive miRNA Delivery to Subcutaneously Implanted Prostate Cancer Cell Line in Mice*—Animal experiments in this study were performed in compliance with the guidelines of the Institute for Laboratory Animal Research, National Cancer Center Research Institute. Seven-week-old male Balb/c athymic nude mice (CLEA Japan, Shizuoka, Japan) were anesthetized by exposure to 3% isoflurane for injections and *in vivo* imaging. Four days ahead of the first CM injection, the anesthetized animals were subcutaneously injected with $5 \times 10^5$ PC-3M-luc cells suspended in 100 μl of sterile Dulbecco's phosphate-buffered saline into each dorsal region. Five hundred μl of CM derived from miR-143-overexpressing HEK293 cells and control cells were daily injected into each tumor from day 0 to 6. For *in vivo* imaging, the mice were administered D-luciferin (150 mg/kg, Promega) by intraperitoneal injection. Ten minutes later, photons from animal whole bodies were counted using the IVIS imaging system (Xenogen) according to the manufacturer's instructions. Data were analyzed using LIVINGIMAGE 2.50 software (Xenogen).

## RESULTS

*Suppression of Prostate Cancer Cell Proliferation by Conditioned Medium Isolated from Non-cancerous Prostatic Cell*—Cell competition is a homeostatic mechanism for the accommodation of an appropriate number of cells in a limited niche or stroma (1). Based on this idea it is possible that the cell competition between normal and abnormal cells frequently occurs in a precancerous state. Of note is that non-cancerous cells suppress cancer cell development by contact-independent interaction (12). For instance, endothelial cells provide the major extracellular heparan sulfate proteoglycan as anti-proliferative signals (12); however, the molecular mechanism by which the other types of cells in a tumor environment associate with cancer cells is not fully understood.

To analyze the mechanism, we treated a hormone-insensitive prostatic carcinoma cell line, PC-3M-luc cells, with a CM from the non-cancerous prostate cell line PNT-2 cells. After a 3-day incubation, the PNT-2 CM inhibited the growth of the PC-3M-luc cells up to ~10% compared with the cell growth treated by fresh culture medium (Fig. 1*A*; compare *lanes 1* and *3*). In contrast, the growth of PC-3M-luc cells incubated in the CM of PC-3M-luc cells themselves showed no inhibitory effect (Fig. 1*A*; compare *lanes 1* and *2*). To determine that the performed treatments did not affect the luciferase activity, we also used the colorimetric MTT assay to measure the cell growth of PC-3M-luc cells. As shown in supplemental Fig. 1*A*, not only luciferase assay but also MTT assay show the inhibition of PC-3M-luc cell proliferation by the addition of PNT-2 cells derived CM, indicating that our treatment did not affect the luciferase activity. These results indicate that the non-cancerous cells may secrete some molecules that can suppress cancer cell proliferation.

In a recent report we showed that miRNAs contained in exosomes are secreted and that their secretion is tightly regulated by neutral sphingomyelinase 2, which is known to hydrolyze sphingomyelins to generate ceramides and trigger the budding